

02

**THE CLOUDSAT MISSION AND THE EOS CONSTELLATION: A NEW DIMENSION
OF SPACE-BASED OBSERVATIONS OF CLOUDS
AND PRECIPITATION**

Graeme L. Stephens¹, Deborah G.Vane², Ronald Boain², Gerald Mace³, Kenneth Sassen³, Zhiem Wang³, Anthony Illingworth⁴ and Ewan O'Connor⁴, William Rossow⁵, Stephen L. Durden², Steven Miller⁶, Richard Austin¹, Angela Benedetti¹, Cristian Mitrescu¹, and the CloudSat Science Team⁷

1. Colorado State University, Department of Atmospheric Science²
Fort Collins, CO 80523-1371
2. Jet Propulsion Laboratory, California Institute of Technology³
Pasadena, CA 91109
3. Department of Meteorology, University of Utah, Salt Lake City
4. Department of Meteorology, University of Reading, UK
5. NASA, Goddard Institute for Space Studies, Columbia, NY
6. Naval Research Laboratory, Monterey, California
7. Refer to the Appendix

Date of Submission: July 31, 2001

Corresponding Author
Graeme Stephens
Colorado State University
Department of Atmospheric Science
Fort Collins, CO 80523-1371
V: (970) 491-8550
F: (970) 491-8166
stephens@atmos.colostate.edu

ABSTRACT

CloudSat is a satellite experiment designed to measure the vertical structure of clouds from space. The expected launch of CloudSat is planned for 2004 and, once launched, CloudSat will orbit in formation as part of a constellation of satellites including NASA's Aqua and Aura satellites, a NASA-CNES lidar satellite (P-C) and a CNES satellite carrying a polarimeter (PARASOL). A unique feature that CloudSat brings to this constellation is the ability to fly a precise orbit enabling the fields of view of the CloudSat radar to be overlapped with the P-C lidar footprint and the other measurements of the EOS constellation. The precision of this overlap creates a unique multi-satellite observing system for studying the atmospheric processes essential to the hydrological cycle.

The vertical profile of cloud properties provided by CloudSat fills a critical gap in the investigation of feedback mechanisms linking clouds to climate. Measuring the vertical profile of cloud properties requires a combination of active and passive instruments, and this will be achieved by combining the radar data of CloudSat with active and passive data from other sensors of the constellation. This paper describes the underpinning science, and gives an overview of the mission, and provides some idea of the expected products and anticipated application of these products. Notably, the CloudSat mission is expected to provide new knowledge about global cloudiness, stimulating new areas of research on clouds including data assimilation and cloud parameterization. The mission also provides an important opportunity to demonstrate active sensor technology for future scientific and tactical applications. The CloudSat mission is a partnership between NASA/JPL, the Canadian Space Agency, Colorado State University, the US Air Force and the US Department of Energy.

1. INTRODUCTION

One of the more stunning features of the visual images we see from space-views of Earth are the cloud systems that move around our planet in the form of quasi-organized large-scale systems (e.g. Rossow and Cairns, 1995). The character and movement of these broad-scale, coherent cloud features are primarily governed by the large-scale atmospheric circulation and, as such, are an essential manifestation of the weather systems of our planet. Motions of synoptic-scale cloud masses, in turn trace the circulation patterns of the atmosphere, and by tracking movements of individual cloud elements we are able to determine the wind fields of the atmosphere (e.g. Menzel, 2000).

These large cloud systems are not mere passive tracers of wide-scale movement of air as they exert an enormous influence on our weather and climate. Clouds are the fundamental element of the atmospheric hydrological cycle, condensing water vapor and eventually forming the precipitation that sustains much of the life on Earth. Clouds also dominate the energy budget of the planet through their effect on the Earth's solar and thermal radiation budgets. Clouds provide a tendency to cool the Earth by reflecting sunlight back to space and they simultaneously warm the Earth by absorbing thermal radiation emitted by the surface and lower atmosphere. By modulating the pole-to-equator variations of both the solar insolation reaching the surface and the radiation emitted to space, and by altering the distribution of heating within the atmosphere, clouds fundamentally influence the global circulations of the atmosphere and oceans.

Despite the fundamental role of clouds in the Earth's climate system, there is much that we do not know. Much of our current global perspective derives from satellite observations primarily in the form of spectral radiances. These offer a unique global view of clouds (as for example provided by the International Cloud Climatology Project (ISCCP), Rossow and Schiffer, 1999) delivering quantitative information about optical properties integrated through the atmospheric column in view. Furthermore, Earth Radiation Budget measurements (e.g. Harrison et al., 1993; Wielicki et al., 1995, Kandel et al., 1998) also provide a measure of the incoming and outgoing radiation at the top of the atmosphere and a measure of the effect of clouds on these outgoing fluxes. Neither data, however, contain direct information about how the radiant energy is distributed vertically within the atmosphere. Both this vertical distribution as well as the horizontal distribution are determined to a large extent by vertical and horizontal variations of

clouds. Understanding how clouds effect these distributions is fundamental to the study of climate variability and change as the atmosphere and oceans respond to these distributions of heating by transporting heat pole-ward in a manner that largely defines the Earth's weather and climate (e.g. Peixoto and Oort, 1992). However, transports in the oceans and atmosphere occur in different ways and on different time scales from one another. The importance of this redistribution of heating is underscored in the study of Glecker et al. (1995) who showed how poorly resolved clouds, through their effects on the surface radiation budget, produces an unacceptable discrepancy in the oceanic poleward transport of heat simulated by a large number of climate models.

The Tropical Rainfall Measurement Mission (TRMM, Simpson et al., 1996) has also advanced our knowledge about how much precipitation falls in the tropical atmosphere. Although it was never a goal of TRMM, using TRMM data we can only crudely estimate the fraction of clouds on Earth that produce precipitation and we cannot estimate within a factor of two what mass of water and ice is contained in these clouds (e.g. Stephens et al., 1998) let alone how much of this water and ice is converted to precipitation. This knowledge is basic to our understanding of the hydrological cycle and the efficiency at which the processes that form this cycle operate and is thus essential for understanding climate variability and change.

The purpose of this paper is two-fold. First, the paper seeks to introduce the reader to a satellite-based cloud experiment (hereafter the CloudSat mission) that aims to provide observations necessary to advance our present state of understanding of the above-mentioned issues. The science that motivates the mission is briefly reviewed in the next section, the science and measurement objectives are stated in section 3 and a general mission overview is provided in section 4. These sections are followed by a description of the space-borne 94 GHz cloud profiling radar (CPR) and its properties (section 5), a brief outline of the measurement requirements (section 6) and an outline of the measurement approach that combines the radar data with other data, as well as the expected products to be derived from the measurements (section 7). Validation is outlined in section 8 and the paper concludes with a summary in section 9. CloudSat is to fly as part of a constellation of satellites formed by EOS Aqua and EOS Aura at each end of the constellation with CloudSat, P-C and PARASOL inserted in the formation between the larger EOS spacecraft (Fig. 1). The second purpose of the paper is therefore to introduce the concept of this constellation (hereafter the EOS constellation).

2.0 THE NATURE OF THE CLOUSAT SCIENCE

2.1 Background

Because of the profound influence of clouds on the water balance of the atmosphere and on the Earth's radiation budget, even small changes in their abundance or distribution could alter the climate response associated with changes in greenhouse gases, anthropogenic aerosols, or other factors associated with global change. Predictions of global warming using climate models forced with a prescribed increase of atmospheric CO₂ are uncertain (Fig. 2a), and the range of uncertainty has not substantially changed much from initial estimates given more than two decades ago. A number of studies have pointed out that one of the main reasons for the continued uncertainty in climate change prediction arises from the difficulties in adequately representing clouds and their radiative properties (e.g. Webster and Stephens, 1983, Cess et al., 1989; Senior and Mitchell, 1993; IPCC, 2001; see <http://www.ipcc.ch>). This point is reinforced in Fig. 2b showing the progression in the prediction of global warming calculated by a single model with CO₂ doubled and with the successive introduction of various feedbacks. The large spread in predicted surface temperature associated with cloud feedback is a consequence of different ways clouds are treated in the same model based on a reasonable range of differing physical assumptions adopted by the model. What is now beginning to emerge from various studies involving coupled ocean-atmosphere models is the even more acute sensitivity of these models to specification of cloud parameters (e.g. Ma et al., 1994).

One step toward unraveling the complex nature of cloud feedback lies in understanding how large-scale atmospheric circulation influences clouds. It is the atmospheric circulation that broadly determines where and when clouds form and how they evolve. Cloud influences, in turn, feed back on the atmospheric circulation through their effects on surface and atmospheric heating, the latter involving a complex combination of radiative and latent heating (e.g. Webster and Stephens, 1983). Thus the basis for understanding this important feedback, in part, lies in developing a clearer view of the association between atmospheric circulation regimes and the cloudiness that characterize these regimes. In more concrete terms, this requires a more quantitative understanding of the relationships between clouds, total diabatic heating and circulation, schematically portrayed in a simple way in Fig 3.

2.2 CloudSat and the connection to Numerical Weather Prediction (NWP)

The approach developed by the cloud-climate research community to explore those aspects of the cloud feedback problem depicted in Fig. 3 relies heavily on the use of general circulation climate models. However, since the connections depicted in this figure are primarily a manifestation of the *weather* systems that form the vast cloud masses that dominate the energy balance of the planet, a fruitful strategy should also embrace numerical weather prediction and related activities. The combination of these prediction models, complete with the extensive assimilation of global meteorological and satellite data and routine analyses to verify the forecasts, provides our most extensive and tested knowledge of the circulation of the atmosphere. Providing the *relevant* observations needed to link this large-scale view of the circulation to cloud heating properties is a key objective of CloudSat. Forging partnerships with major NWP centers, in addition to major climate modeling groups, is an essential ingredient of the CloudSat strategy.

2.3 *The Importance of Cloud Profile Information.*

One of the main reasons model predictions of climate warming vary can be traced to the different ways models specify vertical cloud distributions. Large-scale spatial gradients of heating, set up by large-scale variations of vertical cloud distribution (including the way clouds overlap vertically) have an important influence on the atmospheric circulation and ultimately on model responses to climate forcings. For example, high cloud layers heat the tropical atmosphere by more than 80 Wm^{-2} (relative to clear skies, Stephens, 1999) exerting a dominant influence on the large-scale, 'Hadley' circulation of the atmosphere (Randall et al., 1989) as well as on deep convective cloud systems (Grabowski et al., 2000). The vertical distribution and overlap of cloud layers directly determine both the magnitude and vertical profile of radiative heating (Slingo and Slingo, 1988; Stephens, 2001; and Fig. 4a) which in turn influence many other processes of the models (e.g. Liang and Wang, 1997), notably through the connection between radiative heating, convection and precipitation as illustrated in both model and observational studies (Fowler and Randall, 1994; Parsons et al., 2000).

The assumed vertical distribution of cloud in models also influences precipitation predicted by these models. For example, assumptions about the cloud vertical structure directly influence the extent that the seeder-feeder precipitation mechanism, for example, is assumed to operate in large-scale models (Jakob and Klein, 1999). Figure 4b illustrates the substantial sensitivity of the forecast precipitation on the particular assumption of cloud overlap by showing zonally-averaged precipitation profiles obtained from the forecast model of the European Centre

for Medium- range Weather Forecasts (ECMWF).

These two examples illustrate the importance of cloud profile information on both the radiative budget of the atmosphere and the hydrological cycle even if this information is limited only to profiles of cloud occurrence. Our ability to measure the vertical structure of clouds directly, including the frequency of multiple overlapping cloud layers has, until now, been limited to analyses of data from a few ground-based radar sites. More indirect efforts to obtain a global-scale view of vertical cloud structure rely on observed variations in the profile of water vapor observed in global radiosonde data. Despite these limitations, studies of this type provide useful information about the statistics of cloud vertical structure. For example, Poore et al (1995) and Wang et al. (2000) indicate that overlapping cloud layers occur about 40% of the time in general but that the geographic variability of this statistic is large, with multi-layered cloud frequency ranging from < 10% over deserts and mountains to over 80% in tropical convective regions. Although these global statistics are broadly consistent with those compiled from selected surface sites operating a cloud radar (Mace et al., 1999), they require verification with the more direct measurement approach of CloudSat.

2.4 Cloud water contents and precipitation

The water content of a volume of cloudy air is a parameter fundamental to understanding the role of clouds in the cycling of water through the atmosphere, to how we predict cloud evolution using models, and how we predict other key properties of clouds. For example, various cloud particle growth mechanisms occur at a rate proportional to the water content, including the growth of precipitation-sized drops (e.g. Rogers, 1979). Furthermore, the radiative properties of clouds, such as the cloud albedo and the amount of radiative energy absorbed and emitted, are directly related to water contents and the integrals of water content along the vertical path (e.g. Stephens, 1978).

Models represent clouds as fields of liquid and ice water that are predicted by the time-integration of prognostic water content equations containing terms that are expressions of the parameterizations of various microphysical and turbulent processes (e.g. Sundquist, 1978; Fowler and Randall, 1996, Tiedtke, 1993 and others). The parameterizations contain significant uncertainties that, for the most part, cannot be tested on the global scale. An indication of the extent of the accumulated uncertainty of these parameterizations is provided by the comparisons of the zonal averages of the vertically integrated liquid and solid water contents derived from

many GCM simulations (courtesy of P. Glecker and AMIP II) shown in Fig. 5a. The liquid water path variability amongst models is substantial. Although our ability to provide similar information from observations is crude (Stephens et al., 1998), uncertainties placed on these observations are nevertheless smaller than the model-to-model differences of Fig. 5a. Variations in TOA radiative fluxes (not shown) and precipitation (Fig. 5b) amongst the same models is smaller reflecting the heavy tuning of the model to available observations of these quantities. The fact that the cloud properties are so variable whereas the radiative properties and precipitation are less so underscores serious problems in parameterizations of the pertinent processes that connect radiation, clouds and precipitation.

3.0 CLOUDSAT SCIENCE OBJECTIVES

CloudSat seeks to meet the following specific objectives:

1. *Provide a quantitative evaluation of the representation of clouds and cloud processes in global atmospheric circulation models, leading to improvements in both weather forecasting and climate prediction;* In so doing, CloudSat also seeks to meet the following measurement objectives:
 - Provide the first direct global survey of the vertical structure of cloud systems: This vertical structure is **fundamentally important** for understanding how clouds affect both their local and large-scale atmospheric and radiative environments.
 - Measure the profiles of cloud liquid water and ice water content: These are the quantities predicted by cloud-process and global-scale models alike and determine practically all important cloud properties, including precipitation and cloud optical properties.
2. *Provide a quantitative evaluation of the relationship between the vertical profiles of cloud liquid water and ice content and cloud radiative properties, including the radiative heating by clouds.* The related measurement **objective** is to:
 - Provide coincident profile information on the **bulk** cloud microphysical properties (as **defined** under objective 1) matched to cloud optical properties. Optical properties contrasted against cloud liquid water and ice contents provide a critical test of key parameterizations that enable calculation of flux profiles and radiative heating rates throughout the atmospheric column. To date this type of evaluation can only be carried out using data collected in field programs and from surface measurements limited to a few locations worldwide.

These primary objectives are also augmented by the following secondary science objectives:

3. *Evaluate cloud information derived from other research and operational meteorological spacecraft;* CloudSat data provides a rich source of information for evaluating cloud properties derived from other satellite data including those produced from Aqua as well as cloud information derived from operational sensors as, for example, used by ISCCP. As mentioned below, there are a number of ways CloudSat information will be improved when data from other sensors are combined with the radar. Connecting CloudSat observations to the cloud properties derived from geostationary satellites also serve a number of important purposes. The geostationary information can be used to evaluate and enhance the cloud sample of CloudSat as well as provide a way of projecting the observations of the CloudSat era onto longer times series cloud information provided by ISCCP.
4. *Improve our understanding of the indirect effect of aerosols on clouds by investigating the effect of aerosols on cloud formation;* The potential of aerosol for changing cloud properties and the subsequent influence of these changes on the radiative budget of clouds is referred to as the indirect aerosol forcing (or indirect effect). The aerosol context provided by other constellation measurements (such as by the MODIS on Aqua, the lidar on P-C and the polarimeter on PARASOL), the cloud water, ice and precipitation information of CloudSat, optical property information of MODIS and PARASOL, and the CERES radiative fluxes combine to produce an unprecedented resource for advancing our understanding of this very complex problem.

4.0 MISSION OVERVIEW

The CloudSat mission was selected under the NASA Earth System Science Pathfinder Program (ESSP <http://essp.gsfc.nasa.gov>) and has been confirmed to move into its implementation phase leading to a launch in 2004. Although the original CloudSat concept included the combination of lidar and radar and even precipitation measurements (GEWEX, 1994), the estimated cost of this original concept exceeded the maximum allowable under the ESSP program. The cost constraint imposed by ESSP led to two significant architectural decisions: the involvement of partners who contribute specific portions of the mission thereby reducing the net cost of the mission to NASA, and the use of formation flying with other spacecraft as a way of making near-simultaneous measurements from a combination of sensors.

The extent of the involvement of partners is reflected in the schematic mission overview

portrayed in Fig. 6. The mission was conceived and proposed by the lead author located at Colorado State University where data processing from level 0 to level 3 will be carried out by the Cooperative Institute for Research in the Atmosphere (CIRA). The Jet Propulsion Laboratory (JPL) of the California Institute of Technology is responsible for payload development and project management. The Canadian Space Agency (CSA) is contributing key components and subsystems of the radar. Ball Aerospace provides the spacecraft bus, which is the fifth in the RS2000 line of spacecraft used both for QuikScat and ICESat. Ball Aerospace is also responsible for spacecraft integration and test. The U.S Air Force provides mission ground operations. Validation activities take advantage of ground-based observational sites such as the DOE Cloud and Radiation Test bed (CART) sites as part of the ARM program (Stokes and Schwartz, 1994), NASA and ARM airborne science campaigns, and various national and international university and government research facilities reflected in the science team membership (refer to Appendix A).

4.1 Formation Flying

Formation flying is a navigation strategy involving two or more spacecraft moving in matched orbits and actively maneuvering to maintain a pre-determined geometry with respect to each other. The parameters of this pre-determined geometry are selected to facilitate coordination of complementary measurements taken from each of the spacecraft in the formation. These parameters are monitored and routinely adjusted by small propulsive maneuvers. CloudSat will maintain a formation with respect to two spacecraft, namely Aqua and P-C. The goal is to fly in formation with P-C in such a way as to overlay radar footprints with the lidar footprints at least 50% of the time as well as fly in formation with Aqua such that radar footprints fall in the central few kilometers of the MODIS swath. Because the imaging swath of MODIS on Aqua is so much broader than the lidar footprints of P-C, in practice, CloudSat will control its formation in relation to P-C much more precisely than with Aqua.

The general formation flying concept is illustrated in Fig. 7. Both CloudSat and P-C follow the Aqua spacecraft that is in an orbit synchronized to the World Reference System (WRS-2) grid of ground-tracks. To fly this grid, Aqua uses a sun-synchronous orbit with a 1:30 p.m. Local Mean Time for its ascending node. Aqua's orbit repeats its ground track every 16 days although not precisely owing to orbit perturbations due to atmospheric drag and other lesser effects. As a consequence, Aqua will perform periodic maneuvers to maintain an actual sub-satellite position close to the WRS-2 grid and these maneuvers will be performed whenever Aqua's motion deviates

more than 20 km east or west from the WRS-2 reference thus restoring the Aqua's ground track to within +/-20 km of the reference ground track. This cross-track motion constraint also constrains the deviation of the along-track motion relative to a central position fixed exactly on the WRS-2 grid to 44 seconds back and forth from the central position. This +/-44 seconds deviation in the along-track direction defines Aqua's "control box" relative to the WRS-2 grid as indicated in Fig.7. In practice, Aqua's cross-track deviations are to be controlled relative to the WRS-2 to be better than +/-10 km, well within the +/-20 km requirement reducing the along-track deviation to just +/-22 seconds and creating a smaller control box.

P-C desires to maintain a loose formation with Aqua so that P-C maneuvers are no more frequent than Aqua maneuvers. Thus, P-C defines its formation flying control box of approximately the same dimensions as Aqua's as shown in Fig. 7. By contrast, CloudSat has two sets of formation goals relating to its along track displacement from P-C and Aqua. CloudSat seeks to trail Aqua by less than two-minutes (120 seconds) throughout the CloudSat mission life and will maneuver into a relatively close position just 15-seconds ahead of P-C. CloudSat will then maintain a tight formation with respect to P-C, controlling the cross track motion of the CloudSat spacecraft to within a +/-1 km band relative to the P-C ground track. This is achieved by placing CloudSat in a small circulation orbit, relative to P-C, contained within P-C's control box. This circulation orbit would swing roughly 2.5 seconds forward and backward of a mean position always 15-seconds in front of P-C (See Fig. 7.). Maneuvers to maintain this circulation orbit will be carried out approximately weekly.

4.2 Orbit and Mission Duration

The temporal sampling and global coverage characteristics of CloudSat are dictated by the Aqua orbit which is a sun-synchronous, 705 km altitude orbit with an equator crossing time of 1:30pm. The orbit altitude is significantly higher than that of TRMM, and therefore the sensitivity of the radar is reduced relative to what would be achieved in a preferred lower, TRMM-like orbit. The decision to fly at the altitude of the Aqua orbit was arrived at by weighing the competing the factors of maximizing the radar sensitivity against maximizing the value of synergistic measurements from the EOS constellation.

The CloudSat mission is designed with a two-year lifetime requirement to observe more than one seasonal cycle. There are no anticipated technical reason, however, that prohibit the mission extending beyond 2 years. For example, given the available data on component lifetime and the

current design, the radar can be expected to operate beyond 3 years with an approximate 99% probability.

4.3 Ground-sector Operations

The U. S. Air Force Space Test Program is providing ground operations and is managing communications with the spacecraft. The data will be down-linked several times per day through S-band links as part of the US Air Force SGLS network of receiving stations. CIRA, at Colorado State University (CSU), will handle data processing and distribution of the data for the duration of the mission. The data processing center (DPC) system design is based on the current CIRA satellite earth-station model which has been operational since 1994. CIRA will process all CloudSat level 0 data and higher-level products (i.e. Levels 1 and 2).

All CloudSat Standard Data Product generation software (Level 1 and 2) will be hosted on a software application called the Data Processing and Error Analysis System (DPEAS) (Jones and Vonder Haar, 2001) that currently processes 17 TB of data from various satellites per year. DPEAS is centered on the HDF-EOS format and is based on a parallel—computing environment that has a number of distinct and desirable advantages, including an ability to build redundancy of processors, to accommodate failures and to expand the cluster to respond to growth in data processing needs achieved with easy access to inexpensive scalable computing resources. Data will be made available to the CloudSat Science Team, followed by a release to the scientific community within 6 weeks after the science team has assessed the data and its preliminary validation.

5.0 THE CLOUDSAT CLOUD PROFILING RADAR (CPR)

The CPR provides calibrated backscattered power as a function of distance from the spacecraft. The design has a strong heritage derived from existing ground-based and airborne cloud radars (Mead et. al, 1994; Sadowy et. al, 1997). The choice of radar frequency, namely 94 GHz, is a result of a trade-off between the desire for maximum sensitivity, antenna gain, atmospheric transmission, and radar transmitter efficiency. Sensitivity and antenna gain increase with frequency while atmospheric transmission and transmitter efficiency decrease with frequency. Since a space-based platform sets strong constraints on antenna size, a frequency of 94 GHz provides an optimum compromise between these competing factors. An international frequency allocation at 94 GHz has recently been set aside for spaceborne radar use.

5.1 Radar Reflectivity and the radar equation

In general, the returned power received by a radar after transmitting a power P_t at a wavelength λ is

$$P_r = \left(\frac{P_t G^2 \lambda \theta \phi h}{512(2 \ln 2) \pi R^2} \right) \eta \exp\left[-2 \int_0^R k_{ext}(s) ds\right] \quad (1)$$

where G , θ , ϕ , and h are radar instrument parameters (antenna gain, angle pair defining half power beam width and pulse length respectively) and R is the range to target. The reflectivity η of the target volume follows as

$$\eta = \int_D n(D) \sigma_b(D) dD \quad (2)$$

where σ_b is the backscatter cross-section of each scatterer of size D in the volume and $n(D)$ is the size distribution characteristic of that volume. It is taken to be understood that all quantities are averages over the target volume. With the assumption of Rayleigh scattering, it follows that

$$\eta = \frac{\pi}{4} \frac{K^2}{\lambda^5} Z \quad (3)$$

where Z is referred to as the radar reflectivity factor and $K(=m^2-1/m^2+2)$ is the dielectric factor. Under circumstances of Rayleigh scattering, Z is approximated as

$$Z = \int n(D) D^6 dD \quad (4)$$

For the non-Rayleigh conditions more prevalent at the shorter wavelengths of the 94 GHz radar, (4) can be modified in the form

$$Z_{Mie} = f(D_o) Z_{Ray}(D_o) \quad (5)$$

where D_o is a characteristic size of $n(D)$ and $f(D_o)$ is a simple function of this characteristic size.

The performance requirements placed on the CPR are dictated by the science objectives and flow-down science requirements (briefly described in the next section). Based on our current understanding of cloud reflection, the requirement placed on the sensitivity of CPR, expressed as the minimum detectable reflectivity factor (hereafter MDS), is -26 dBZ at end of mission, a 70 dB dynamic range, and a calibration accuracy of 2 dBZ before launch (and goal of 1.5 dBZ). The MDS of the CloudSat radar is expected to be between -28 to -29 dBZ during the earlier phase of

the mission and this sensitivity is required given the weak nature of the scattering by cloud particles. By comparison, the Tropical Rainfall Measuring Mission (TRMM) Precipitation Radar (PR) has a sensitivity of approximately +20 dBZ.

With this sensitivity, the CloudSat CPR detects the majority of clouds that significantly affect the radiation budget and critical elements of the water budget of the atmosphere. Assessment of the impact of those clouds missed by the CPR on these budgets is an ongoing research activity. The instantaneous radar footprint is 1.4 km, and along-track averaging will be performed on various scales to produce cloud profiles with varying levels of detectability. The averaging scenarios adopted to produce these different profiles are currently being analyzed.

Cloud and precipitation information provided by the radar is to be recorded with a 500-m vertical resolution between the surface and 30 km. The radar footprint equates to an antenna diameter of approximately 2 meters which is the maximum size that fits the shroud of the launch vehicle. The antenna pattern requires that the spacecraft be pointed with an accuracy of 0.5° to minimize direct surface reflections and contamination from sidelobes.

5.2 94 GHz attenuation

The exponential factor in (1) represents the two-way attenuation of the radar pulse as it propagates through the atmosphere. At 94 GHz, this attenuation results from absorption by gases (chiefly water vapor), liquid water droplets and precipitation-sized particles. Tables 1a and 1b provide some idea of the attenuation expected under typical atmospheric conditions and contrast the attenuation at 94 GHz against the attenuation of a radar operating at 14 GHz. The quoted attenuation by water vapor is the two-way attenuation through the entire column from the satellite altitude to the stated level. This attenuation can be adequately corrected using profile information derived from operational analyses whereas the attenuations by cloud droplets and precipitation (table 1b) are included in the design of relevant retrieval algorithms.

5.3 The 94 GHz reflectivity characteristics of clouds

The proliferation of cloud radar systems world-wide over the past decade has led to a broader understanding of the radar reflection properties of various types of clouds than was available at the time of the early formulation of CloudSat. Cloud radars now operate routinely or quasi-routinely at a number of surface sites worldwide (e.g. Moran et al., 1998, Clothiaux et al., 1999). Cloud radars also operate on various research airborne platforms. Measurements collected over a number of years from these research radars provide a way of systematically comparing

cloud radar reflectivity properties to cloud information derived from other sensors operated alongside the radars. Data collected over many years reveal how the reflectivity of clouds vary over several orders of magnitude. The range of reflectivities is exemplified by the time-height radar reflectivity cross-section shown in Fig. 8. The profiles shown were measured by an airborne cloud radar flown on the NASA DC-8 over a convective cloud complex and illustrate the cloud radar representation of convective precipitation, stratiform precipitation and overlying layers of ice clouds. The reflectivity factor ranges from below -30 dBZ around the edges of the upper ice layers to in excess of ± 20 dBZ in heavier precipitation.

Profile data of the type presented in Fig 8, when accumulated from a large number of flights and many hours of surface measurements, provide a data-base for establishing the general reflectivity characteristics of different cloud types. Examples of this accumulation of aircraft and surface radar data are shown in Figs. 9a and b in the form of cumulative probability distributions (CPD) of low-level water clouds. The CPDs of Fig. 9a are constructed from approximately 30,000 airborne reflectivity profiles of marine stratus and stratocumulus observed off the coast of California and over the Southern Pacific Ocean in the vicinity of New Zealand. Shown for comparison is a similar reflectivity CPD derived from more than 17,000 profiles of continental layered clouds observed by the MMCR operated over the DOE ARM CART site. The CPD of low level water clouds seen by ground based lidar as a function of radar reflectivity is displayed in figure 9b, obtained from an analysis of 6600 hours of coincident radar/lidar data over a 15 month period in the UK. This figure, in contrast to Fig. 9a, suggests that for a sensitivity of -28 dBZ the radar detects only 25% of the low level water clouds detected by the lidar and thus underscores the need to continue these kinds of sensitivity analyses and underscores the importance of the other data of the constellation.

Similar kinds of composite analyses applied to cirrus cloud radar data highlight the different nature of the radar reflection by these types of clouds. Figure 10 (upper panel) is an example of the joint statistics obtained from combined lidar and radar measurements of tropical thin cirrus (adapted from Mitrescu and Stephens, 2001) collected over a 3-month period as part of the ARM Nauru Tropical Western Pacific radiation site. These statistics are in the form of the optical depth of tropical cirrus derived from a lidar transmission and the radar reflectivity averaged over the layer of cirrus. The data do not represent all cirrus observed during that time but only thin cirrus that do not fully attenuate the lidar. The middle and lower panels show the

fraction of these clouds missed by a radar with equivalent MDS and vertical resolution properties of CloudSat. This fraction is expressed in terms of optical depth (middle panel) and TOA outgoing longwave flux (lower panel). Based on the analyses presented in this figure, the limit of cirrus detection by a CloudSat-like radar generally lies in the range of optical depths between 0.1-0.4 although there is variability about this range (upper panel). At Nauru, there is a prevalence of thin cirrus that lies below the detection threshold of the CloudSat-like radar (37% of all thin cirrus cases) but these cirrus have minimal impact on the water budget of the upper troposphere (average paths less than 1 gm^{-2}) and on the TOA longwave flux (average OLR effects of 5 Wm^{-2}).

Far less is known about the reflectivity of the different types of underlying surfaces that will be encountered by an orbiting space-borne 94 GHz radar. What limited information is available indicates that surface reflectivity typically varies as a function of surface type and condition as influenced by vegetation, soil moisture, and snow depth (among other factors) over land and surface wind speed over oceans (Ulaby and Dobson, 1989). Characterization of the 94-GHz surface reflectivity in terms of relevant surface properties is one area of emerging research that can be expected to be promoted through the CloudSat project.

5.4 Cloud Detection Algorithm

The cloud geometric profile product (refer to Table 2 and related discussion below) is derived from the radar reflectivity data (level 1b). The goal of the profile algorithm is to maximize the identification of hydrometeor echoes while minimizing the occurrence of false alarms. The approach developed is referred to as the significant echo mask (SEM) algorithm which follows the method of Clothiaux et al. (1995; 2000). The SEM algorithm identifies radar echoes in the profile of returned power that lie significantly above the background noise and thus contain, to high probability, hydrometeors within the given volume. The SEM method requires as input the power returned, nominally an average of 644 pulses for two combined radar footprints, and the Gaussian-like background system noise. The initial criterion for a significant return is a reflectivity three standard deviations above a background threshold deduced from near-by returns. To improve detection of weak returns, a statistical approach that effectively increases the separation between signal and noise is also implemented. The approach compares the reflectivity from a given range

bin with that of its neighbors and identifies weakly reflecting, but spatially persistent, hydrometeor layers.

Figure 11 demonstrates an example of this method highlighting the approach applied to ARM cloud radar (MMCR) data. The radar reflectivities shown in the upper panel of Fig.11 are the actual MMCR reflectivities at the full radar sensitivity and volume resolution of that radar, whereas the bottom two panel shows the reflectivities derived after applying the SEM degraded to the CloudSat resolution and sensitivity.

6.0 OVERVIEW OF THE CloudSat MEASUREMENT REQUIREMENTS

One of the key objectives of the mission is to be able to provide information sufficient for determining the contribution of clouds to the radiative heating of the atmosphere. This contribution, and the radiative fluxes that determine it, are to be derived indirectly using models initialized with the level-2 products output from the CloudSat algorithms summarized in Table 2.

Accuracy requirements placed on the level 2 products were established by tracing these requirements back to a requirement established for the radiative heating and related radiative fluxes. Although measurement requirements for top-of atmosphere (TOA) fluxes are documented (e.g. Wielicki et al., 1996), it is neither a straightforward nor obvious task to relate these TOA flux requirements to heating rates. The approach developed to establish the heating rate requirement connects variations of cloud radiative heating to changes in observable quantities, chosen to be atmospheric temperature and precipitation since measurement requirements exist for these parameters. The relation between cloud radiative heating rates, temperature and precipitation was established using two general circulation models (Schneider and Stephens, 1996). This further provided a way of connecting TOA fluxes to cloud radiative heating, thereby providing a connection to the documented TOA and surface flux requirements of CERES. Using these flux requirements represents a more tangible way of establishing accuracy requirements on optical depth, liquid and ice water contents, and minimum radar detection thresholds (Miller and Stephens, 2001).

The results of the abovementioned studies may be summarized as follows.

- (i) GCM sensitivity studies suggest that changing in-cloud radiative heating by an amount of 1K day^{-1} over a 1 km layer leads to predicted changes in the precipitation rate in the tropics of about 10% and changes to atmospheric temperature globally of 1-2 K. The latter are

consistent with present capabilities to measure atmospheric temperature, and the precipitation changes are slightly below with the measurement capabilities presently understood for TRMM. The changes to temperature and precipitation are also consistent with the along-track estimation of instantaneous longwave excitant fluxes within 5-10 W.m^{-2} at the top and bottom of the atmosphere.

- (ii) TOA longwave fluxes, derived by comparing simulations that contain $\pm 20\%$ differences in cloud optical depth and liquid water content, compared to control simulations are within $\pm 5 \text{ W.m}^{-2}$ of the control simulations (Miller and Stephens, 2001).
- (iii) Based on realistic assumptions for the particle sizes of ice and water clouds, a radar with a minimum sensitivity of -28 dBZ will miss some optically thin high clouds and a higher fraction of low clouds (note also Figs. 9 and 10). Although we do not know these statistics on the global scale, we estimated that a radar-only system operating with a minimum sensitivity of -28 dBZ will detect approximately 90-95% of all ice mass and approximately 80% of the water mass. However, when combined with other radiance observations (such as available from MODIS), many of the undetected low water clouds will also be counted, and further improvement for ice content is expected with the addition of P-C lidar observations. Overall, our best estimate is that the clouds missed by CloudSat will impact the in-cloud radiative heating by less than 1K day^{-1} per km. Studies that provide a clearer understanding of the detection thresholds of the CloudSat radar, and the impacts of these thresholds on the related science, continue to be a focus of ongoing research.
- (iv) The clouds missed by the radar lead to an underestimate of the instantaneous TOA and surface longwave fluxes, largely by missing some fraction of low clouds. When detection of low thin clouds by the radar is augmented by radiance data from Aqua, it is expected that these longwave flux errors will reduce to approximately 5 W.m^{-2} .
- (v) The corresponding visible optical depths of clouds undetected by a radar-only observing system operating with a -28 dBZ MDS varies with particle size. Assuming particle sizes typical of those observed, the threshold radar detection is about $\tau \approx 1-3$ for low-level water clouds and $\tau \approx 0.1-0.4$ for ice clouds (although this varies according to the cloud microphysics).

7.0 THE CLOUDSAT MEASUREMENT APPROACH AND EXPECTED PRODUCTS

The principal products of the CloudSat mission are summarized in Table 2. The primary product is the level 1b calibrated, range-resolved radar reflectivities. The key level 2 product is the cloud profile information derived from the SEM algorithm (referred to as 2B-geoprof). Two classes of level 2 products are noted. The standard data products are those that provide information necessary to meet the objectives for the mission. The experimental products provide supplementary information leading to an overall enhancement of the science of the mission (for example, at this time, precipitation is an experimental product). The important, practical difference between these two classes of products is that the standard products will be processed at the DPC and made available for distribution to the general scientific community as described above. The experimental products will be produced and archived by individual scientists; whether these products eventually transition to standard products and make their way accordingly to the central archive will be assessed by the science team.

Level 2 data, archived at the pixel level, are also to be averaged over space and time to produce a series of level 3 products (not listed in Table 2). A discussion of the Level 3 products, general sampling characteristics of the mission and related sampling errors will be described in another paper, although general information about the types of sampling errors expected for the time-space-mean CloudSat products can be found in GEWEX (1994). Level 2 products also include a subset of MODIS and AMSR radiance (level 1) data, as well as a number of selected (level 2) MODIS and CERES products specifically matched to the CloudSat radar ground track that will be used primarily for diagnostic and comparative studies.

Table 2 also identifies the principal source of sensor data necessary to provide the science products. All Level 2 products are derived from radar reflectivities although some products, as indicated, require additional information. For example, liquid water and ice content products can be derived from reflectivities directly but are improved with the addition of optical depth information (discussed in the following section, see also Fig.12). The list of experimental products also anticipates combining CloudSat data with Aqua sensor data, lidar data of P-C and data from other members of the EOS constellation. This experimental list of products is expected to grow and underscores the value and unique opportunity provided by the EOS constellation.

7.1 Cloud Classification

The unique value of cloud radar measurements is the more or less direct connection between radar reflectivity and cloud water and ice content. While the physical basis for this connection is straightforward, as discussed below, variability introduced by cloud microphysical properties introduce a source of ambiguity. Although we will attempt to relieve this ambiguity using approaches discussed in the next section, we also plan to develop a cloud classification product to help identify the types of clouds being observed in part used for diagnostic purposes and in part to provide a means for selecting certain parameter sets in the algorithms. The classification algorithm for identifying cloud type and precipitation will be derived from the information expected to be available (cloud radar, imaging radiance data and lidar observations) and a prototype version of this algorithm is described by Wang and Sassen (2001a). Adaptation of this algorithm using CloudSat and other EOS constellation data is in progress.

7.2 Theoretical basis for cloud retrievals using combined sensor data: Introductory Concepts

The measurement approach and the algorithms developed for retrieving liquid and ice water contents are predicated on exploiting the different properties of active and passive observing systems. The benefits of combining these different measurement approaches into a single cloud-observing system has been demonstrated for more than 20 years using measurements from both aircraft and ground-based lidar, radar and radiometer systems (e.g. Platt et al., 1997; Matrosov et al., 1992; Mace et al., 1999; Austin and Stephens, 2001; and Sassen and Mace, 2001; among others). The bases for the CloudSat algorithms are consequently mature, with versions of some of the algorithms currently in quasi-operational use today in the DOE-ARM program.

The value of combining multi-sensor data for retrieving cloud physical information is conveniently and simply demonstrated in the following way. The Level 2b geoprof cloud radar reflectivity Z , under circumstances of Rayleigh scattering, follows as

$$Z \rightarrow \int n(D) D^6 dD \rightarrow N_0 D_0^6 \rightarrow w D_0^3 \quad (6)$$

where D is the particle diameter, $n(D)$ is the cloud particle number density, N_0 is the total number concentration and w is the desired liquid or ice water content – information of principal relevance to the science goals of CloudSat. D_0 in (6) refers to a ‘characteristic’ particle size relevant to $n(D)$.

As noted above and elsewhere (e.g. Atlas et al., 1995; Brown et al., 1995) reliable estimates

of w do not follow directly from measurements of Z alone as additional information about the mean particle size or the relation between mean particle size and w is required. One source of this information is the cloud optical depth τ obtained from measurements of reflected sunlight. Optical depth relates to w and r_e according to (e.g. Stephens, 1978)

$$\tau = \int dz \int n(r) \pi r^2 Q_{\text{ext}} dr \rightarrow \int w/r_e dz \rightarrow \text{LWP}/r_e \quad (7)$$

where Q_{ext} is the extinction efficiency, r_e is the effective radius (related to D_o) and LWP is the liquid (or ice) water path (discussed previously in relation to Fig. 5a). Optical depth information is to be provided from MODIS radiance data matched to the radar field of view (Table 2).

It follows from (6) and (7) that the radar reflectivity, when integrated vertically through the cloud layer, (i.e. $IZ = \sum Z$), and optical depth provide independent information about liquid or ice water path (LWP, IWP) and mean particle size (Austin and Stephens, 2001; Matrosov et al., 1992). Austin et al. (2001) demonstrate this approach in the retrieval of cloud liquid water content based on both airborne and surface data. In an analogous manner, Matrosov et al. (1992) have demonstrated this concept applied to the retrieval of ice water content and Fig. 12 below also highlights the advantages of this approach for retrieval of IWC compared to other approaches.

7.3 The Algorithm Approach

Water and ice content algorithms conceptually start with the definition of the CloudSat observing system expressed in a convenient, although heuristic form:

$$y = f(x, b) + \varepsilon, \quad (8)$$

where y is the measurement vector, f is the ‘forward model’ representing the underlying physical basis of the algorithm, x is the desired vector of parameters to be retrieved, b is a vector of unretrieved ancillary parameters and ε is the measurement error. The basic purpose of the CloudSat algorithms is to invert (8) to retrieve x and its related error given y , the measurement error and some assumption as to the form of f and related parameters b . In general, a number of complicating factors arise when actually implementing this inversion procedure. These factors generally include large errors in y , uncertainties on the form of f and related parameters, and forms of f that are not readily invertible or lead to unstable and/or non-unique inversions. Many Earth-science retrieval problems, including those specific to CloudSat, suffer from these difficulties (e.g. Twomey, 1977). Furthermore, the CloudSat algorithms are required to be flexible so as to include

(in principle) varying types of information from combinations of different sensor data.

The CloudSat algorithms under development are required to meet the following general properties:

- Have a sound and documented physical basis (that is, the function f is determined from physical principles, as in (4) and (5), and errors on f are to be quantifiable)
- Have flexibility to allow for addition of varying sources of information (i.e. y , x and f are to be extendable)
- Provide an associated, detailed error analyses including detailed breakdown of component errors (i.e. the contribution to the error in x due to y , f and b)
- Offer diagnostic measures of retrieval quality, in addition to error, including some idea of the information content of the relevant measurements in relation to the given product (i.e. the extent that the inversion requires constraints and the extent to which these constraints infiltrate the solution).

Implementation of the operational algorithms proceeds along a formal estimation theory approach popularized in atmospheric remote sensing by Rodgers (2000), among others. The advantage of this approach is the formality it introduces into the problem of retrieval as well the framework it provides for combining multi-sensor data. The method also requires a disciplined approach to the estimation of system errors, providing not only quantifiable product errors but also an error component breakdown that guides the strategy for product validation (described below) and eventual product improvement. This method has been demonstrated in application of the lidar inversion problem (Stephens et al., 2001), cloud optical depth and particle size (Miller et al., 2000), radar retrieval of precipitation under conditions of attenuation (L'Ecuyer and Stephens, 2001), and in the context of CloudSat-like retrievals of cloud water using cloud radar combined with measurements of reflected solar radiation in the form of cloud optical depth (Austin and Stephens, 2001). Work on the retrieval of ice cloud properties combining cloud radar data and MODIS radiances is underway.

7.4 Challenges and Opportunities

Data collected from past measurement activities, as well as data to be collected up to and beyond launch, guide the development of radar algorithms and understanding of the synergy of multi-sensor data combined with radar observations. Although substantial progress has occurred, there remain scenarios where significant ambiguities exist in interpreting observations and where

further understanding is required. Likewise, there are a number of unexplored areas that present the research community with exciting opportunities for developing new observational approaches and providing new scientific information. Some of these areas of research include:

- The continued evaluation of the sensitivity of the CloudSat radar and how cloud detection may be augmented by the other sensors of the EOS constellation: This evaluation must include quantification of the effects of under-detection expressed in terms of both the water budget and radiative budgets of clouds. Although the observing thresholds of the radar, expressed above in terms of optical depth, are consistent with observations reported in the literature, these threshold properties do vary with cloud particle size, in particular, and thus with different cloud types.
- The transition from cloud to precipitation: Whereas the presence of drizzle in clouds as an initial stage in the development of precipitation benefits the problem of detection, particularly for boundary-layered clouds, it also complicates the estimation of cloud liquid water (e.g. Fox and Illingworth, 1997). A number of cloud-radar studies suggest that drizzle in low clouds can be identified using simple radar thresholding approaches (Frisch et al., 1995) or combinations of reflectivity and cloud optical depth (Austin et al., 2001). Despite the emerging ability to discriminate drizzle occurrence, retrieval methods that provide quantitative information about cloud LWC in the presence of drizzle have not been developed. CloudSat provides an opportunity to address this observing problem through a combination of radar data with other satellite radiance data, including the microwave radiance data provided by AMSR.
- Properties of mixed-phase clouds: Super-cooled liquid water obviously coexists with ice, and detection of these mixtures, not to mention quantifying the water contents of each phase, remains an important and particularly challenging problem, not only from the perspective of observations but also from the perspective of parameterization of these processes in global models (e.g. Rotstajn et al., 2000). The cloud radar data, combined with other data of the constellation, such as the depolarization information from the lidar and polarimetric reflectances from PARASOL, provides an opportunity to focus some attention on both the observational challenges associated with mixed-phase clouds as well as on the parameterization of the mixed phase processes in global models.
- Categorization and quantification of precipitation: Solid and liquid precipitation is readily detected by the CloudSat radar. Liquid precipitation exceeding about $10 \text{ mm}\cdot\text{hr}^{-1}$ at the surface

will fully attenuate the space-borne 94 GHz radar in the lowest 1 to 2 km of the vertical profile (Table 1b). L'Ecuyer and Stephens (2001) introduced a 94 GHz radar rainfall algorithm and examined the quality of the precipitation information retrieved using synthetic radar data simulated using the Tropical Rainfall Measurement Mission (TRMM) GPROF data base as input (Ohlsen et al., 1996). They demonstrated that 94 GHz radar data can provide meaningful estimates of surface rainrate to about 3 mm.hr^{-1} , beyond which the rain-rate retrievals suffer from significant attenuation ambiguity. They also showed that inclusion of path attenuation information extends the validity of the precipitation information to almost 10 mm.hr^{-1} . Research is continuing on possible ways of dealing with attenuation, precipitation validation efforts are planned associated with AMSR validation activities.

8.0 THE CLOUDSAT VALIDATION PLAN

The evaluation of both the standard and experimental products is an important focus of ongoing research activities that can be expected to continue prior to and after launch. The intent of these activities is:

1. To determine the calibration accuracy of the radar, thereby verifying the output of the level 1b radar algorithm that produces calibrated radar reflectivity profiles.
2. To determine the location accuracy of the radar footprint to enable the merging of CloudSat data with other data sets
3. To evaluate the CloudSat radar sensitivity and to validate the cloud profile product and cloud detection statistics. Emphasis must continue in the evaluation of the detection characteristics of the CloudSat radar and of how cloud detection is augmented by the other sensors of the EOS constellation.
4. To quantify both random and bias errors estimated by the retrieval methods. The sources of these two errors types include: *Model errors* associated with the way observations are modeled in the retrieval approach. *Measurement error* related to instrument performance, calibration, noise, etc. *Data-base errors* due to uncertainties in *a priori* data-bases used to constrain non-unique solutions (e.g. ambiguities associated with attenuated radar reflectivities etc) or *uncertainties* in data bases used to assign model parameters are an often overlooked, additional source of retrieval error.

A number of specific activities are planned to quantify these errors and characterize the CloudSat observing system. Many of these activities are being carried out prior to launch whereas

other activities will be required throughout all phases of the mission.

Sensor Calibration and footprint location: The calibration of the radar provides an overall uncertainty attached to the individual reflectivities. The CloudSat radar calibration plan includes a routine and detailed system calibration both prior to launch and in flight, vicarious calibration associated with surface returns from the ocean, and direct measurement comparisons with independently calibrated airborne radar volume matched to the space-borne radar. The expected absolute calibration accuracy is 1.5-2 dBZ. Knowledge of the footprint location will be confirmed on orbit using the ocean-land variation of surface reflectivities as the radar field of view crosses coastlines. This approach is expected to provide an independent way of locating the radar footprint with an accuracy of $\leq 800\text{m}$.

Detection: The SEM detection algorithm is essentially a threshold algorithm with a carefully tuned noise threshold. This tuning will be worked on before launch using available data from aircraft flights as well as cloud radar data from ARM. Assessment of the detection algorithm will continue to be a focus of the validation efforts of the project. The performance of the CloudSat detection algorithm will be assessed by statistically comparing against long term surface measurements and, when possible, aircraft measurements volume-matched to the CloudSat radar measurements.

Ground Truth – the objective of ground truth measurements is to confirm the total retrieval error (bias plus random) from all sources. For the case of 2B-LWC and 2B-IWC products, ground truth requires independent data obtained from (say) cloud physics probes that offer a more direct (and usually more accurate) measure of the relevant quantities being evaluated. Unfortunately, there is generally no ‘absolute’ ground truth especially since it is difficult to match the smaller volumes sampled by the direct measurements to the larger volumes sampled by the radar. Although difficult to quantify, ground truth exercises are essential elements of validation and are the only way to estimate the difficult-to-determine systematic retrieval errors. Post-launch ground-truth efforts applied to the actual CloudSat products are currently being planned.

Component Error Analyses: This activity attempts to quantify individual error components of the retrieval system, in particular focusing on model and data base errors. For clouds and precipitation, the most significant sources of retrieval error are typically those attached to the retrieval forward model f , related parameters b , and *a priori* data bases implicit to the retrieval. For the CloudSat algorithm, these analyses make use of a variety of data sources including

currently archived cloud physics data obtained from past aircraft measurement programs worldwide (e.g. Austin et al., 2001) and rely heavily on the systematic measurement activities of ARM. An example of this type of analyses is provided in the study of Vali and Haimov (1998) who confirm the theoretical relation between measurements of (one-way) attenuation as a function of cloud liquid water content using a **horizontally pointed radar** flown on the University of Wyoming King Air in marine stratocumulus. The coefficients of the simple linear relationship between attenuation and liquid water content (the uncertainties attached to these coefficients) represent specific model parameters used in cloud liquid water retrievals as described by Austin and Stephens (2001).

Consistency analyses: For this activity, the retrieved information is compared to other information that in one way or other can be correlated with the cloud information in question. One example is provided in the form of a comparison of cloud radar based liquid water path information matched and compared to LWP inferred from MODIS optical properties and others are noted under (ii) below .

The specific strategy proposed to carry out these steps include:

- (i) Application of algorithms to synthetic data for which the actual cloud information is known:
An example of **this approach** is described in the study of Sassen et al. (2001b) who employ an explicit cirrus microphysical model to simulate time--evolving radar reflectivities, lidar backscatter and optical depths (Fig. 12a and b). This information is provided to various ice water content algorithms, which are then compared to the model predicted IWC as shown in Fig. 12c. These comparisons then provide a way of assessing the algorithms and how other factors not explicitly included in the algorithms affect their performance. In the example shown, the more common empirical Z-IWC algorithms lack the robustness of both the lidar-radar (Wang and Sassen, 2001b) and radar-optical depth algorithms that capture microphysical variation from cloud type to cloud type as indicated by the cases shown for different cloud temperatures.
- (ii) Comparison of products derived from different algorithms based on different kinds of data inputs: For example, the ice water contents derived from simpler CloudSat-like algorithms of the type noted in Fig. 12 that use reflectivity data primarily can be compared to equivalent information derived from algorithms that use either additional radar data such as reflectivity at a different frequency (Sekelsky et al, 1999) or reflectivity data plus Doppler moment data

(Clothiaux et al., 2000) or entirely different sensor data as in the example of microwave radiometer cloud liquid water path data (e.g. Austin et al., 2001).

- (iii) Application of the algorithms to surface based radar data that are then subsequently evaluated using information matched to the radar volumes obtained from airborne platforms with necessary cloud microphysical sensors.
- (iv) Similar to (iii) but using aircraft radar and radiometer data matched to measurements from *in situ* aircraft sensors of relevant cloud parameters in a manner similar to that reported in the study of Austin et al. (2001).
- (v) Similar to (iv) matching aircraft *in situ* data with satellite data after launch.

The CloudSat validation plan benefits from the systematic measurement programs of ARM that focused on the use of surface remote sensors as well as systematic measurements planned for selected sites within Europe and Japan. The validation plan also benefits from regular aircraft radar measurement activities within USA, Japan and Europe, the measurement capabilities at number of universities (Sassen et al., 2001a) and cloud field program activities representing targets of opportunity planned in the coming years. CloudSat also has begun to link to the validation activities of P-C as well as to the validation activities planned for Aqua.

9.0 SUMMARY

CloudSat is designed to measure the vertical structure of clouds and precipitation from space and does so through the first space-borne flight of a 94 GHz cloud profiling radar. Not only will this mission stimulate important new research on clouds and precipitation, but it will also provide an important demonstration of the 94 GHz radar technology in a space-borne application. The expected launch year of CloudSat is 2004 and, once launched, CloudSat will come into formation as part of a constellation of satellite P-C and PARASOL. CloudSat will maintain a formation that enables overlapping the field of view of the CloudSat radar in a precise way with other measurements of the constellation creating a unique, multi-satellite, observing system particularly suited for studying the atmospheric processes of the hydrological cycle.

CloudSat employs a measurement and algorithm approach that combines radar information with radiance data obtained from other sensors of the constellation. Information derived from this combination, summarized in Table 2, includes detailed vertical profile information about the water and ice contents of clouds, the occurrence of precipitation and quantitative information about precipitation. CloudSat will provide a large and unique ensemble of these properties

providing new knowledge about clouds and precipitation and the connection of clouds to the large scale motions of the atmosphere, offering probing tests of global climate and weather forecast models as well as cloud resolving models and related parameterizations. As such, CloudSat will provide new ways of examining relationships between clouds and other properties of the atmosphere that are important in establishing the cloud-climate feedbacks.

10. ACKNOWLEDGMENTS

The research described in this paper was carried out at a number of institutions, including the Jet Propulsion Laboratory, California Institute of Technology, under a contract with the National Aeronautics and Space Administration (NASA). This research was also supported by NASA Contract NAS 5-99237, Calif. Inst. of Tech/Jet Propulsion Lab Contract #1212032 and Calif. Inst. of Tech/Jet Propulsion Lab #961158 at Colorado State University.

11. REFERENCES

- Atlas, D. A., S. Y. Matrosov, A. J. Heymsfield, M-D Chou, and D. B. Wolff, 1995: Radar and radiation properties of ice clouds. *J. Appl. Met.*, **34**, 2329-2345.
- Austin, RT. And G.L. Stephens, 2001; Retrieval of Stratus cloud microphysical parameters using millimetric radar and visible optical depth in preparation for CloudSat, Part I: Algorithm Formulation, to appear *J. Geophys. Res.*
- Austin, R.T., G.L Stephens, S.D. Miller, S.M. Sekelsky, F. Li and Q. Min, 2001; Retrieval of Stratus cloud microphysical parameters using millimetric radar and visible optical depth in preparation for CloudSat, Part II: Algorithm Evaluation, to appear *J. Geophys. Res.*
- Brown, P.R.A., A. J. Illingworth, A. J. Heymsfield, G. M. McFarquhar, K. A. Browning, and M. Gosset, 1995: The role of spaceborne millimeter-wave radar in the global monitoring of ice cloud. *J. Appl. Met.*, **34**, 2346-2366.

- Cess, R. D., et al., 1989: Interpretation of cloud-climate feedback as produced by 14 atmospheric general circulation models. *Science*, **245**, 513-516.
- Clothiaux, E. E., M. A. Miller, B. A. Albrecht, T. P. Ackerman, J. Verlinde, D. M. Babb, R. M. Peters, and W. J. Syrett, 1995: An evaluation of a 94 GHz radar for remote sensing of cloud properties, *J. Atmos. Oceanic Technol.*, **12**, 201-229.
- Clothiaux, E. E., K. P. Moran, B. E. Martner, T. P. Ackerman, G. G. Mace, T. Uttal, J. H. Mather, K. B. Widener, M. A. Miller, and D. J. Rodriguez, 1999: The Atmospheric Radiation Measurement program cloud radars: operational modes. *J. Atmos. Ocean. Tech.*, **16**, 819-827.
- Clothiaux, E. E., T.P. Ackerman, G.G. Mace, K.P. Moran, R.T. Marchand, M.A. Miller and B.E. Martner, 2000; Objective determination of cloud heights and radar reflectivities using a combination of active remote sensors at the ARM CART sites, *J. Appl. Meteorol.*, **39**, 645-665.
- Frisch, A.S., C.W. Fairall and J.B. Snider, 1995; Measurements of stratus cloud and drizzle parameters in ASTEX with Ka-band Doppler radar and microwave radiometer, *J. Atmos. Sci.*, **52**, 2788-2799.
- Fowler, L.D and D. A Randall, 1994; A Global Radiative-Convective Feedback, *Geophys. Res. Letters*, **21**, 2035-2038
- Fowler and Randall, 1996; Liquid and ice cloud microphysics in the CSU General Circulation Model. Part I: Model description and simulated microphysical processes, *J. Climate*, **9**, 489-529.
- Fox, N. I., and A. J. Illingworth, 1997: The retrieval of stratocumulus cloud properties by ground-based cloud radar. *J. Appl. Met.*, **36**, 485-492.

- GEWEX 1994; *Utility and feasibility of cloud profiling radar*, International GEWEX Project Office, World Climate Research Programme, Pub. Series #10.
- Gleckler, P. J. ; Randall, D. A. ; Boer, G. ; Colman, R. ; Dix, M. ; Galin, V. ; Helfand, M. ; Kiehl, J. ; Kitoh, A. ; Lau, W. ; Liang, X. -Z. ; Lykossov, V. ; McAvaney, B. ; Miyakoda, K. ; Planton, S. ; Stern, W. 1995: Cloud-radiative effects on implied oceanic energy transports as simulated by atmospheric general circulation models, *Geophys. Res. Lett.*, 7, 791-794.
- Grabowski, W. W., J.-I. Yano, M. W. Moncrieff, 2000: Cloud resolving modeling of tropical circulations driven by large-scale SST gradients. *J. Atmos. Sci.*, 57, 2022-2039.
- Harrison, E. F., P. Minnis, B.R. Barkstrom and G. G. Gibson, 1993; Radiation budget at the top of the atmosphere, in *Atlas of satellite observations related to global change*, Gurney, Foster and Parkinson (Eds), 19-38.
- L'Ecuyer, T. S., and G. L. Stephens, 2001: An estimation-based precipitation retrieval algorithm for attenuating radars. To appear in *J. Appl. Met.*
- Liang, X-Z and W-C Wang, 1997; Cloud Overlap effects on GCM Climate Simulations, *J. Geophys. Res.*, 102, 11039-11047.
- Jakob, C., and S. A. Klein, 1999: The role of vertically varying cloud fraction in the parameterization of microphysical processes in the ECMWF model. *Quart. J. Roy. Meteorol. Soc.*, 125, 941-965.
- Jones, A. S., and T. H. Vonder Haar, 2001: Overview of an HDF-EOS-based parallel data computing environment for multisensor satellite data merger and scientific analysis. Preprints, 17th conference on Interactive Information, and Processing Systems (IIPS) for Meteorology, Oceanography, and Hydrology, 14-19 January, Albuquerque, NM, Amer. Meteorol. Soc., 329-332.

Kandell, R., M. Viollier, P. Raberanto, J. P. Duvel, L. a. Pakhomov, V. A. Golovko, A. P.

Trishchenko, J. Mueller, E. Raschke, and R. Stuhlmann, 1998: The ScaRaB Earth radiation budget dataset. *Bull. Am. Met. Soc.*, **79**, 765-783.

Ma, C.C, C.R. Mechoso, A. Arakawa and J. Farrara, 1994; Sensitivity of a Coupled Ocean-Atmosphere Model to Physical Parameterizations, *J. Clim.*, **7**, 1883-1896.

Mace, G. G., C. Jakob, and K. P. Moran, 1999: Validation of hydrometeor prediction from the ECMWF model during winter season 1997 using millimeter wave radar data. *Geophys. Res. Lett.*, **25**, 1645-1648.

Matrosov, S. Y., T. Uttal, J. B. Snider, and R. A. Kropfli, 1992: Estimation of ice cloud parameters from ground-based infrared radiometer and radar measurements. *J. Geophys. Res.*, **97**, 20675-20683.

Mead, J. B., A. L. Pazmany, S. Sekelsky, and R. McIntosh, 1994: Millimeter wave radars for remotely sensing clouds and precipitation. *Proc. IEEE*, **82**, 33-47.

Menzel, P. W., 2000: Cloudtracking with satellite imagery: From the pioneering work of Ted Fujita to the present. *Bull. Am. Met. Soc.*, **82**, 33-47.

Miller, S. D., G. L. Stephens, C. K. Drummond, A. K. Heidinger, and P. T. Partain, 2000: A Multisensor diagnostic cloud property retrieval scheme. *J. Geophys. Res.*, **105**, 19,955-19,971.

Miller, S. D., and G. L. Stephens, 2001: CloudSat instrument requirements as determined from ECMWF forecasts of global cloudiness. In press: *J. Geophys. Res.*

Mitrescu, C. and G. L. Stephens, 2001: A new method for determining cloud transmittance and optical depth using the ARM Micro-Pulsed Lidar. Accepted: *J. Atmos. Ocean. Tech.*

- Moran, K.P., B.E. Martner, M.J. Post, R. A. Kropfli, D.C. Welsh and K. Widener, 1998; An unattenuated cloud-profiling radar for use in climate research, *Bull. Amer. Met. Soc.*, **79**, 443-455.
- Olson, W. S., C. D. Kummerow, G. M. Heymsfield, L. Giglio, 1996: A method for combined passive-active microwave retrievals of cloud and precipitation profiles. *J. Appl. Met.*, **35**, 1763-1789.
- Parsons, D.B., K. Yoneyama, and J-L Redelsperger, 2000; Evolution of the tropical western Pacific atmosphere-ocean system following the arrival of a dry intrusion; *Quart. J R. Meteorol. Soc.*, **126**, 517-548.
- Peixoto, J.P. and A. H. Oort, 1992; *Physics of Climate*, AIP Press, 520pp
- Platt, C.M.R., S. A. Young, P. J. Manson, G. R. Patterson, S. C. Marsden, R. T. Austin, and J. Churnside, 1997: The optical properties of equatorial cirrus from observations in the ARM pilot radiation observation experiment. *J. Atmos. Sci.*, **55**, 1977-1996.
- Poore, K. D., J. Wang, and W. B. Rossow, 1995: Cloud layer thicknesses from a combination of surface and upper-air observations. *J. Clim.*, **8**, 550-568.
- Randall, D. A., Harshvardhan, D.A. Dazlich and T.G. Corsetti, 1989: Interactions among radiation, convection and large-scale dynamics in a general circulation models. *J. Atmos. Sci.*, **46**, 1943-1970.
- Rodgers, C.D., 2000; *Inverse Methods for Atmospheric Sounding: Theory and Practice*; World Sci Pub., Series on Atmospheric, Oceanic and Planetary Physics, Vol 2, 238pp
- Rogers, R. R., 1979: A Short Course in Cloud Physics (2nd Ed.), Pergamon Press, 235 pp.
- Rossow, W. B., and B. Cairns, 1995: Monitoring changes of clouds. *Clim. Change*, **31**, 305-347.

- Rossow, W. B., and R. A. Schiffer, 1999: Advances in understanding clouds from ISCCP. *Bull. Am. Met. Soc.*, **80**, 2261-2287.
- Rotstajn, L. D. B.F. Ryan, and J.J Katzfey, 2000; A scheme for calculation of the liquid fraction in mixed-phase stratiform clouds in large-scale models, *Mon. Wea. Rev.*, **128**(4), 1070-1088.
- Sadowy, G. A., R. E. McIntosh, S. J. Dinardo, S. L. Durden, W. N. Edelstein, F. K. Li, A. B. Tanner, W. J. Wilson, T. L. Schneider, and G. L. Stephens, 1997: The NASA DC-8 airborne cloud radar: Design and preliminary results. Proceedings: *International Geoscience and Remote Sensing Symposium*, Singapore, August 1997.
- Sassen, K., J. M. Comstock, Z. Wang, and G. G. Mace, 2001a: Cloud and aerosol research capabilities at FARS: The Facility for Atmospheric Remote Sensing. *Bull. Amer. Meteor. Soc.*, **82**,1119-1138.
- Sassen, K, and G. G. Mace, 2001: Ground Based Remote Sensing of Cirrus Clouds, in "Cirrus", D. Lynch, K. Sassen, D. O'C. Starr, and G. L. Stephens, Eds. Oxford University Press, 168-195.
- Sassen, Wang, Mace, Stephens, Matrosov and Khvorostyanov, 2001b: Evaluating radar algorithms for cirrus cloud property retrieval using cloud model predictions. Submitted to *J. Appl. Met.*
- Schneider, T. L., and G. L. Stephens, 1996: Climatically relevant clouds as seen by a space-borne radar, lidar, and submillimeter-wave radiometer. Presented at the *Intl. Rad. Symposium: Current Problems in Atmospheric Radiation*, August 19-24, 1996, University of Alaska, Fairbanks.

- Sekelsky, S.M., W.L. Ecklund, J.M. Firda, K.S. Gage and R.E. McIntosh, 1999; Particle size estimation in ice-phase clouds using multifrequency radar reflectivity measurements at 95,33 and 2.8 GHz, *J. Appl. Meteorol.*, **38**,5-28.
- Senior, C. A., and J.F.B. Mitchell, 1993: Carbon dioxide and climate: The impact of cloud parameterization. *J. Clim.*, **6**, 393-418.
- Simpson, J., C. Kummerow, W.K. Tao and R.F. Adler, 1996: On the Tropical Rainfall Measuring Mission (TRMM) . *Meteorol. Atmos. Phys.*, **60**, 19-36.
- Slingo, A., and J. M. Slingo, 1988: Response of a general circulation model to cloud long-wave radiative forcing, Part I: Introduction and initial experiments. *Q. J. Roy. Met. Soc.*, **114**, 1027-1062.
- Stephens, G. L., 1978: Radiation Profiles in extended water clouds: Parameterization Schemes, *J. Atmos. Sci*, **35**, 2123-2132.
- Stephens, G. L., 1999: Radiative Effects of clouds and water vapor. Chapter 3.1: Water vapor. *Global Energy and Water Cycles*. Eds. Browning/Gurney, Cambridge University Press., 71-90.
- Stephens, G. L., 2001, Cirrus, Climate and Global Change, In *Cirrus* in "Cirrus", D. Lynch, K. Sassen, D. O'C. Starr, and G. L. Stephens, Eds. Oxford University Press., 433-448.
- Stephens, G. L., C. Jakob and M. Miller, 1998; Atmospheric ice- a major gap in understanding the effects of clouds on climate, in *GEWEX News*, **8(1)**, 1-8.
- Stephens, G. L., M. Vaughan, R. J. Engelen, and T. L. Anderson, 2001: Toward retrieving properties of the tenuous atmosphere using space-based lidar measurements. In Press: *J. Geophys. Res.*

- Stokes, G. M., and S. E. Schwartz, 1994: The Atmospheric Radiation Measurement (ARM) Program: programmatic background and design of the cloud and radiation test bed. *Bull. Am. Met. Soc.*, **75**, 1201-1221.
- Sundquist, H. 1978; Parameterization scheme for nonconvective condensation, including prediction of cloud water content, *Quart. J. Roy. Meteorol. Soc.*, **104**(441): 677-690.
- Tiedtke, M., 1993; Representation of clouds in large-scale models, *Mon. Wea. Rev.*, **121**, 3040-3061.
- Twomey, S., 1977; *Introduction to the Mathematics of inversion in remote sensing and indirect measurements*, Elsevier, 243pp.
- Ulaby, F. T., and M. C. Dobson, 1989; *Handbook of Radar Scattering Statistics for Terrain*. Massachusetts: Artech House.
- Vali, G., R. D. Kelly, J. French, S. Haimov, D. Leon, R. E. McIntosh, and A. Pazmany, 1998: Finescale structure and microphysics of coastal stratus. *J. Atmos. Sci.*, **55**, 3540-3564.
- Wang, Z., and K. Sassen, 2001a: Cloud type and property retrieval using multiple remote sensors. *J. Appl. Meteor.*, **40**, (in press).
- Wang, Z., and K. Sassen, 2001b: Cirrus cloud microphysical property retrieval using lidar and radar measurements: I. Algorithm description and comparison with *in situ* data. *J. Appl. Meteor.*, (submitted).
- Wang, J-H., W.B. Rossow and Y-C. Zhang, 2000: Cloud vertical structure and its variations from a 20-year global raw insonde dataset. *J. Climate*, **13**, 3041-3056.
- Webster, P. J. and G. L. Stephens, 1983: Cloud-radiation interaction and the climate problem, In *The Global Climate*, (Houghton, Ed), CUP, 63-78

Wielicki, B. A., R. D. Cess, M. D. King, D. A. Randall, E. F. Harrison, 1995: Mission to planet Earth: Role of clouds and radiation in climate. *Bull. Am. Met. Soc.*, **76**, 2125-2153.

Wielicki, B. A., B. R. Barkstrom, E. F. Harrison, R. B. Lee, G. L. Smith, and J. E. Cooper, 1996: Clouds and the Earth's Radiant Energy System (CERES): An Earth Observing System experiment. *Bull. Am. Met. Soc.*, **77**, 853-868.

12. Appendix A: CloudSat Science Team Members

Tom Ackerman	Pacific Northwest Laboratory, USA
Howard Barker	Atmospheric Environment Service, Canada
Frank Evans	University of Colorado, USA
Jurgen Fischer	University of Berlin, Germany
David Hudak	Atmospheric Environment Service, Canada
Anthony Illingworth	University of Reading, United Kingdom
Hiroshi Kumagai	Communications Research Laboratory, Japan
Fuk Li	Jet Propulsion Laboratory, USA
Zhanqing Li	University of Maryland, USA
Gerald Mace	University of Utah, USA
Sergey Matrosov	NOAA Environmental Test Laboratory and University of Colorado, USA
Teruyuki Nakajima	University of Tokyo, Japan
Markus Quante	GKSS Research Center, Germany
David Randall	Colorado State University, USA
William Rossow	NASA Goddard Institute for Space Studies, USA
Kenneth Sassen	University of Utah, USA
James Spinhirne	NASA Goddard Space Flight Center
Graeme Stephens, Principal Investigator	Colorado State University, USA
Ron Steward	Atmospheric Environment Service, Canada
Cal Swift	University of Massachusetts, USA
Jacques Testud	Université de Versailles St-Quentin, France

Andre van Lammeren	Royal Netherlands Meteorological Institute, Netherlands
Deborah Vane	Jet Propulsion Laboratory, USA
Thomas Vonder Haar	Colorado State University, USA
Steven Walter	Aerojet Corporation, USA
Bruce Wielicki	NASA Langley Research Center, USA
David Winker	NASA Langley Research Center, USA

Captions to Figures

Fig. 1 The concept of the EOS—PM constellation and its members.

Fig 2 (a) The responses of various coupled-ocean-atmosphere general circulation models to an imposed doubling of CO₂. (b) The response of a single climate models to an imposed doubling of CO₂ as different feedbacks are systematically added in the model (adapted from Senior and Mitchell, 1993)

Fig. 3 A schematic depiction of the main elements of the Cloud–feedback problem. The links between the boxes indicate processes that are the key to the way the feedbacks are established.

Fig. 4. (a) Vertical profiles of cloud radiative heating rate (K/day) differ due to the different location and thickness of cloud layers (shaded, and adapted from Slingo and Slingo, 1988). The net column flux divergence is +45 Wm⁻² (left panel), +12 Wm⁻² (center panel) and +3 Wm⁻² (right panel) defined relative to clear skies. (b) Zonal mean large-scale precipitation rate for the first time step of a T63L31 integration with the sub-grid precipitation model using maximum-random (solid), maximum (dashed) and random (dotted) cloud overlap.

Fig. 5 (a) Comparison of the zonally averaged liquid-plus-solid water paths derived from the GCM simulations submitted to AMIP II. (b) Comparison of the zonally averaged precipitation derived from the same suite of models of (a).

Fig. 6 CloudSat Mission Overview

Fig. 7 A schematic of the orbit control boxes of three PM constellation satellites indicating the relation between each other. In this depiction, CloudSat maintains a tight formation with respect to the P-C lidar spacecraft.

Fig. 8: Time–height cross-section of radar reflectivity as measured by a downward-looking 94 GHz radar on NASA’s DC-8 research aircraft.

Fig. 9 (a) Examples of reflectivity probability density functions derived from many thousands of reflectivity profiles collected from boundary-layer stratiform clouds. (b) Same as (a) but for surface radar observations over the UK.

Fig. 10 The joint optical depth-radar reflectivity statistics obtained derived from the Nauru ARM MMCR surface radar and the ARM micro-pulsed lidar (upper). The probability distribution of cloud optical depth (middle) and of TOA OLR (lower panel) for all thin cirrus missed by a CloudSat-like radar the cloud radar (Mitrescu and Stephens, 2001).

Fig. 11. Example of the SEM algorithm applied to ARM surface radar data. In (a), the full resolution radar data are shown and (b) the radar profiles derived after applying the SEM to identify clouds and assign a reflectivity to the identified reflectivity volume are shown.

Fig. 12 The upper two panels show the time-height cross-sections of cloud ice water content and the radar reflectivities predicted by an explicit cirrus cloud microphysical models for the case with mid-cloud temperature of -61°C . Retrieved ice water paths from various radar algorithms compared to modeled ice water paths for three cloud simulations differentiated by cloud temperature. The tau-Z algorithm refers to the CloudSat-like algorithm that uses MODIS and CloudSat CPR data.

Table 1a: Calculated two-way attenuation (in dB) of a TRMM-like PR radar (14 GHz) and a CloudSat-like radar (94 GHz) derived for a path from the top of the atmosphere to three representative levels

McClatchey Profile	14 GHz			94 GHz		
	10 km	5km	0.5 km	10km	5km	0.5 km
Tropical	0.015	0.047	0.293	0.121	0.550	5.454
Mid-lat Summer	0.014	0.043	0.231	0.114	0.476	4.084
Mid-lat Winter	0.012	0.038	0.137	0.099	0.352	1.820
Sub-arctic winter	0.011	0.037	0.118	0.091	0.321	1.312

Table 1b: Characteristic attenuation of water droplet clouds, ice crystals and precipitation. Two way attenuation in cloud is derived from the values given multiplied by a given water or ice content of the cloud and the two-way geometric path length through clouds. Two-way attenuation in precipitation is derived via

$$\sigma_P^D = k_P R^\gamma \text{ (dB/km)}$$

multiplied by the two way geometric path length through precipitation. Values of σ_P^D are given for specified rainrates.

Liquid	10 cm			14 GHz			94 GHz		
	-8C	10C	20C	-8C	10C	20C	-8C	10C	20C
n	8.94	9.02	8.88	5.39	6.89	7.44	2.53	3.04	3.34
k	1.8	0.9	0.063	3.03	2.78	2.41	1.23	1.75	2.04
Im (-K)	0.013	0.0069	0.0051	0.0063	0.035	0.027	0.217	0.177	0.153
kc*	0.011	0.0056	0.0042	0.239	0.135	0.102	5.72	4.68	4.05
Ice	10 cm			14 GHz			94 GHz		
		-20C			-20C			-20C	
n		1.78			1.78			1.78	
k		0.0002			0.0007			0.003	
Im(-K)		9.0E-5			0.0003			0.001	
kc*		7.0E-5			0.0011			0.029	
Rain	10 cm			14 GHz			94 GHz		
kp		0.00000			0.014			0.744	
		4							
gamma		1			1.21			0.734	
0.1 mm/hr!		4X10 ⁻⁷			9X10 ⁻⁴			0.137	
1 mm/hr!		4X10 ⁻⁶			1.4X10 ⁻²			0.744	
10 mm/hr!		4X10 ⁻⁵			0.277			4.033	

* in dB/km/g/m³

! in dB/km

Table 2: List of CloudSat products, the principal inputs and properties

1. Standard Product ID	Description	Principal Inputs	Characteristics and references
1A-Aux	Auxiliary data and raw CPR data	Digital Elevation maps, space craft ephemeris	
1B-Radar reflectivities	Calibrated radar reflectivities	Radar power, calibration factors	500m vertical resolution
2B-Geoprof	Cloud geometric profile – expressed in terms of occurrence and reflectivity (significant echoes), also includes (gas) attenuation correction profile information	1B radar reflectivities, MODIS cloud- mask product	500m vertical resolution Marchand and Mace (2001)
2B-Cloud classification	8 classes of cloud type, including precipitation identification and likelihood of mixed phase conditions	Radar and other data from the EOS constellation	Wang and Sassen (2001)

2B-Tau	Cloud optical depth by layer	2B-Geoprof and MODIS radiances	$\tau > 0.1$, 20% accuracy (goal)
2B-LWC	Cloud liquid water content	2B-Geoprof and 2B-Tau	500m and 50%
2B-IWC	Cloud ice water content	2B-Geoprof and 2B-Tau, temperature	500m +100% to -50%
2B- Fluxes/heatin g rates	Atmospheric radiative fluxes and heating rates	2B-Geoprof, 2B-Tau, 2B- LWC/IWC	Resolve longwave fluxes at TOA and surface to ~ 10 Wm^{-2} and equivalently in cloud heating to $\sim \pm 1$ K/day/km
2. Auxiliary Data			
AN- ModMask	MODIS cloud mask product	Subsetting to \pm - 35 km about the Aqua nadir track	

AN-ModRad	MODIS radiances	Radiances from 23 of the MODIS channels subsetting as above	
AN-State variables	Forecast model state variables Subsetting along the CloudSat ground track	The subsetting details are currently under study	
AN-AMSR	AMSR radiances		
3. Experimental Products			
Precipitation	Quantitative precipitation	2B-Geoprof and AN-AMSR radiances	
Cloud Phase	Discrimination of ice and liquid	2B-Geoprof, P-C lidar, MODIS radiances	

Cloud Microphysics	Droplet size profiles, number concentrations	2B-Geoprof, 2B-Tau, P-C lidar, MODIS radiances	
-----------------------	---	---	--

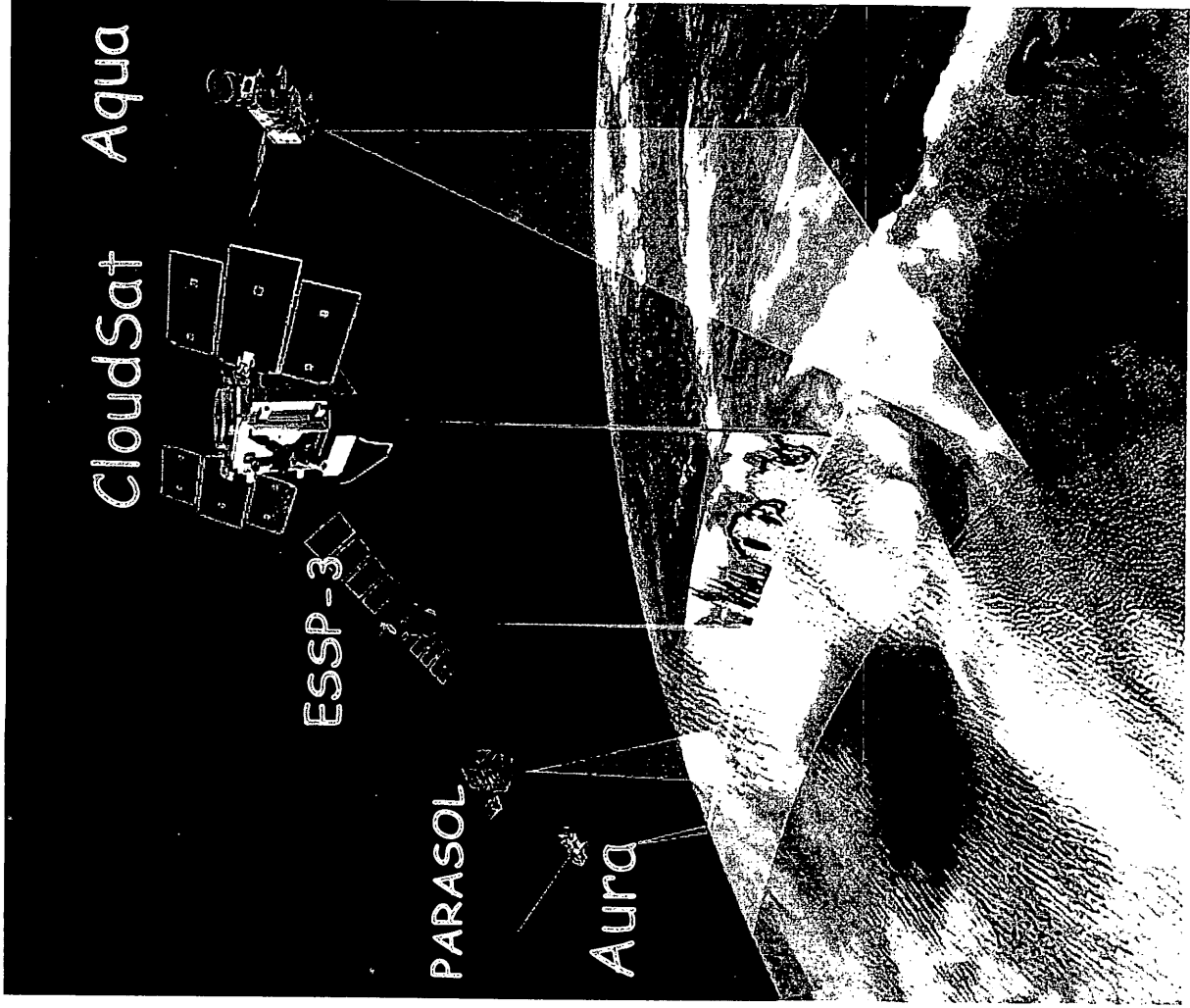


Fig. 1 &
Cover proposal

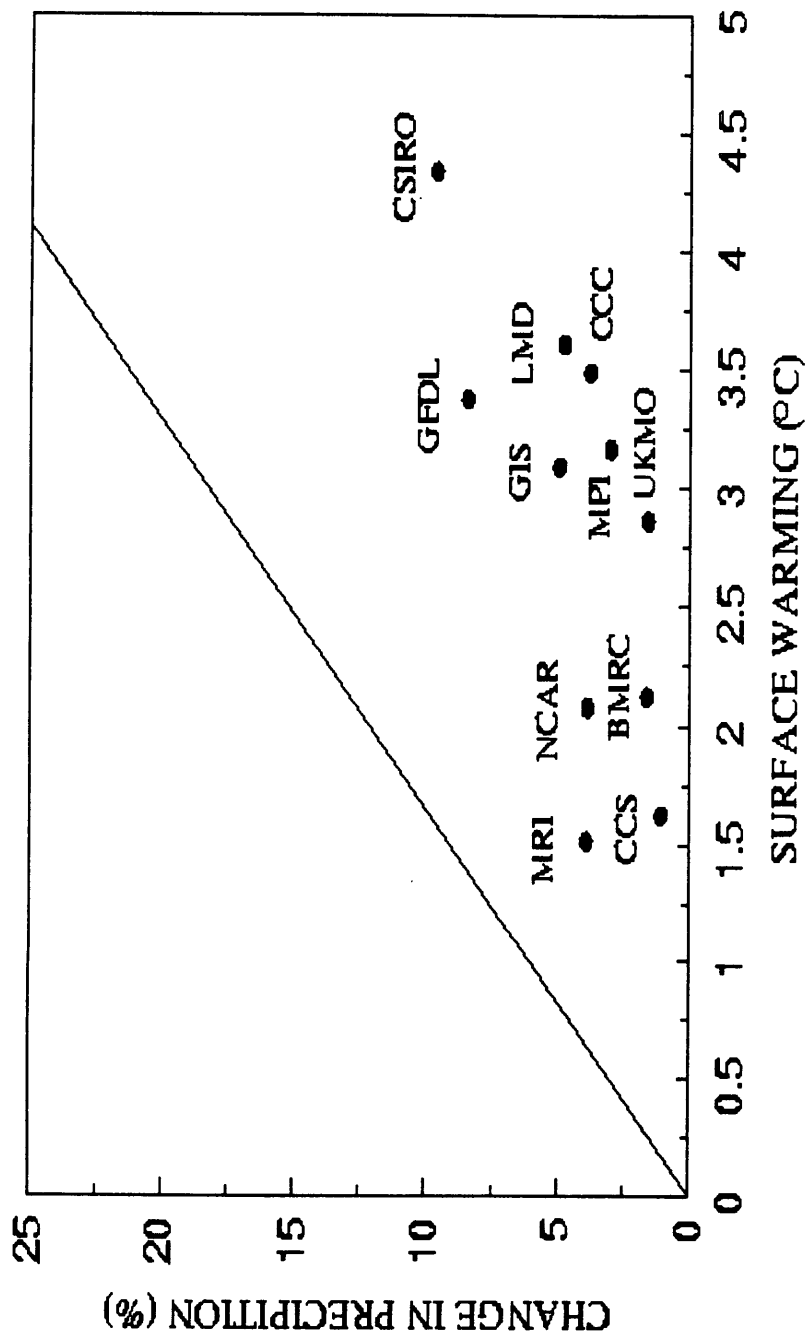


Fig. 2a

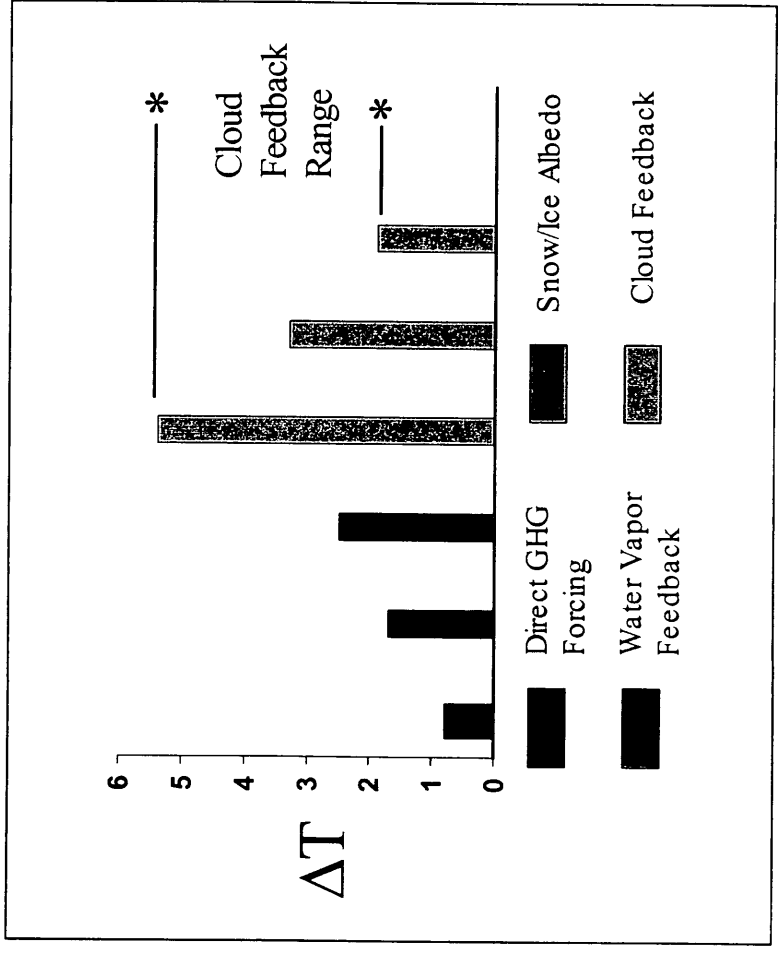


Fig. 2b

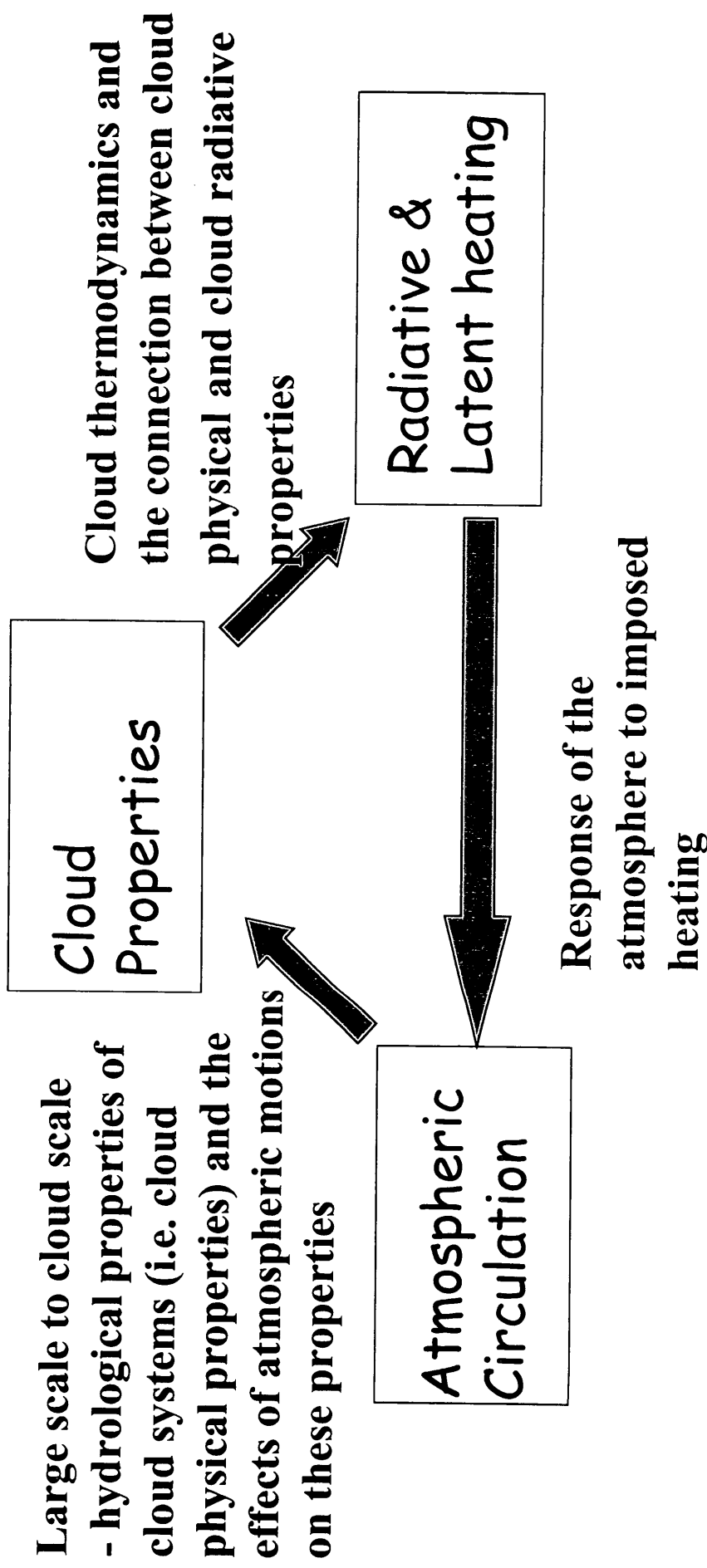
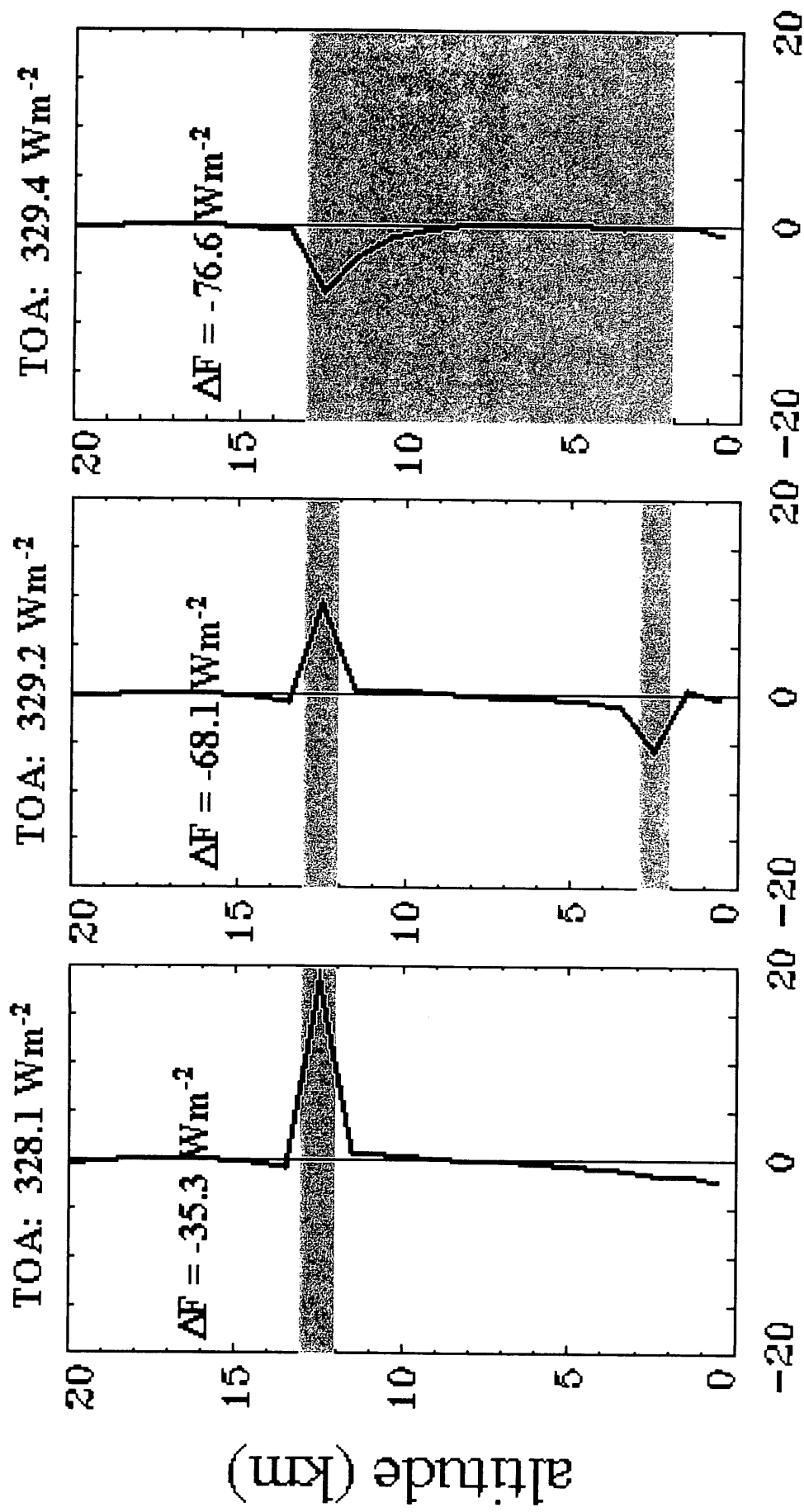


Fig. 3



radiative heating (K/day)

Fig. 4a

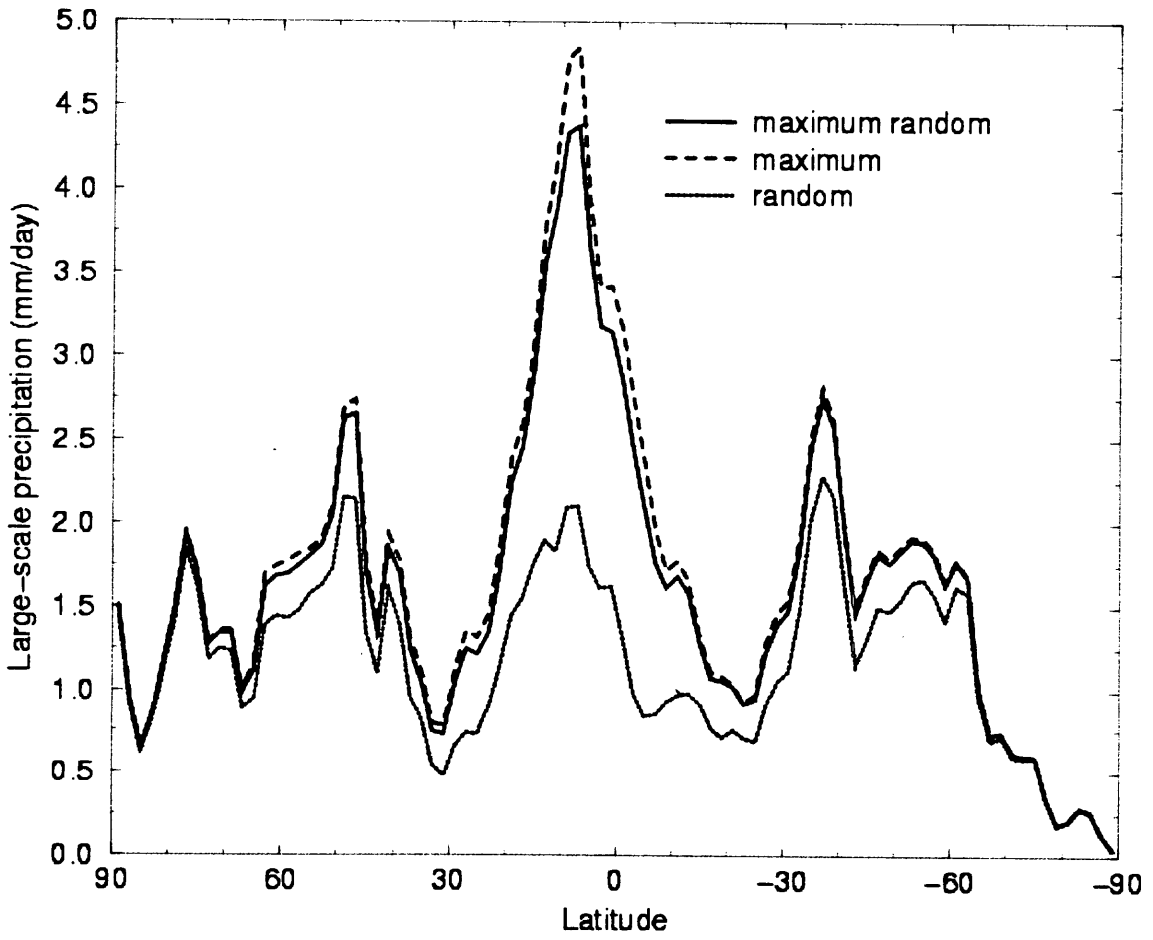
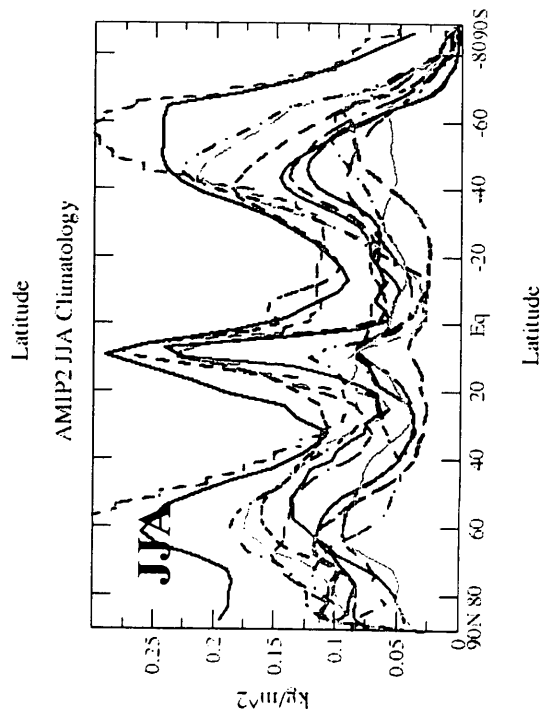
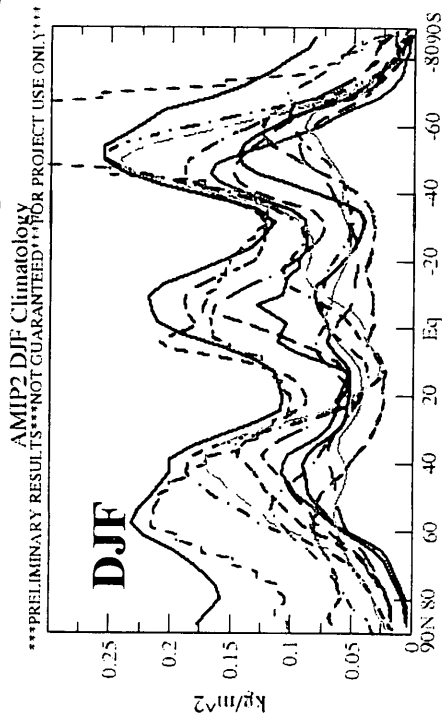


Fig. 4b

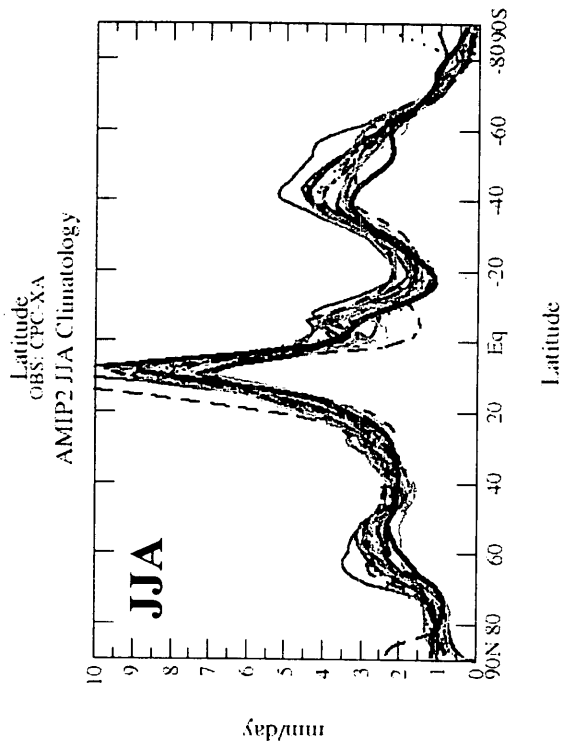
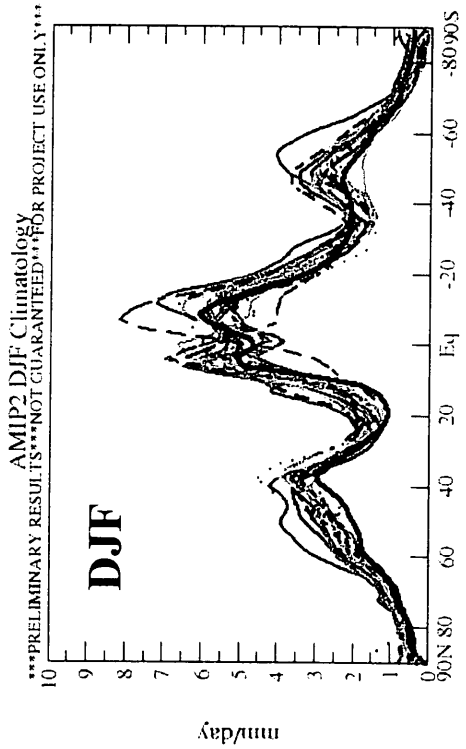
Vertically integrated cloud water (liquid and solid phase)



Mon Apr 30 07:56:14 2001

(a)

Total precipitation rate



Mon Apr 30 07:44:48 2001

(b)

Fig. 5

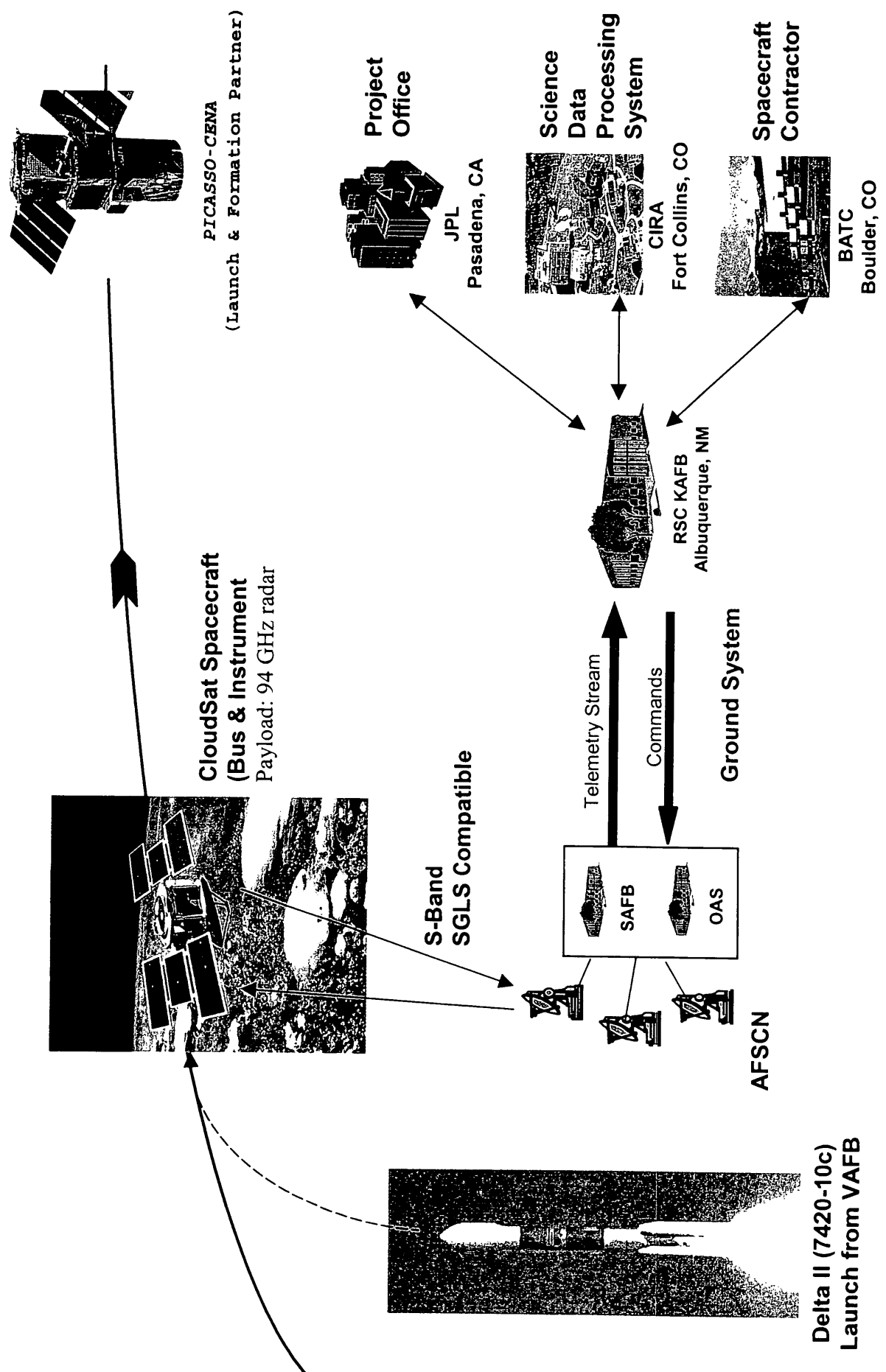


Fig. 6

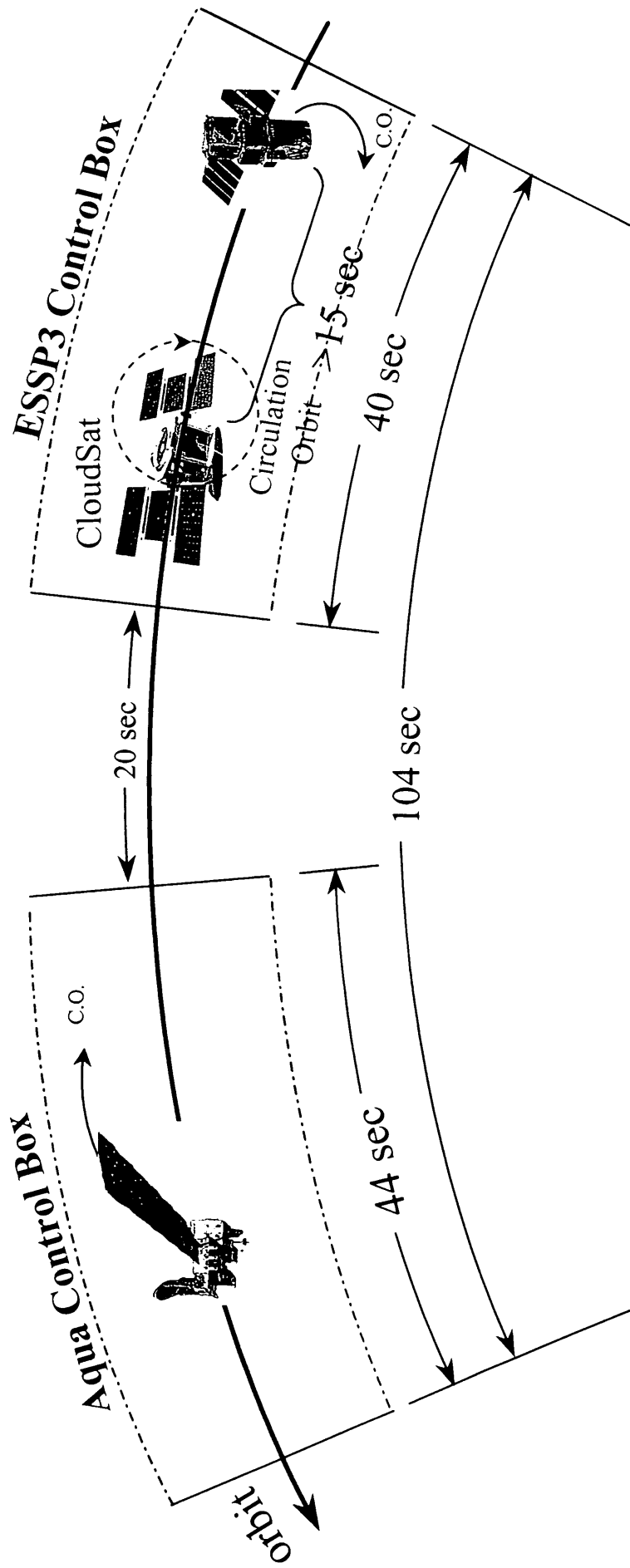


Fig. 7

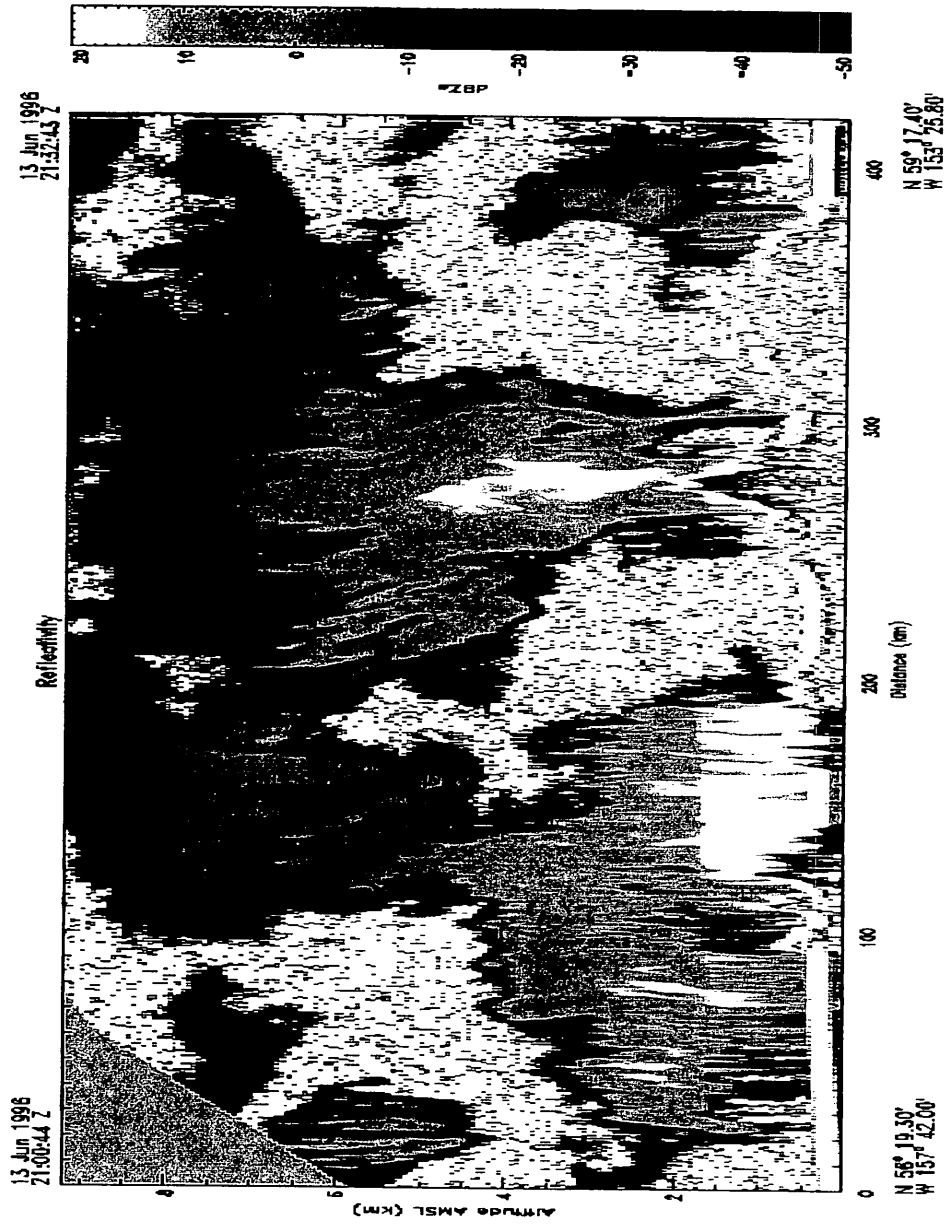


Fig. 8

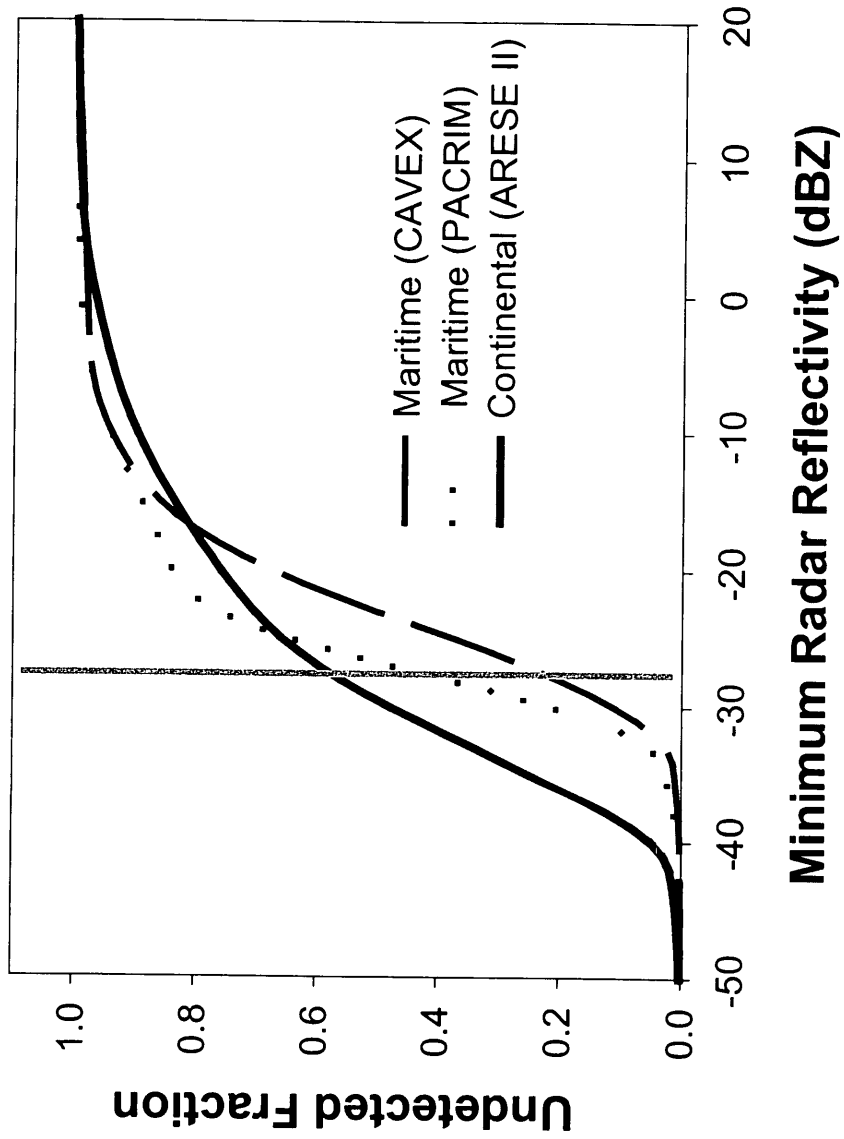


Fig. 9a

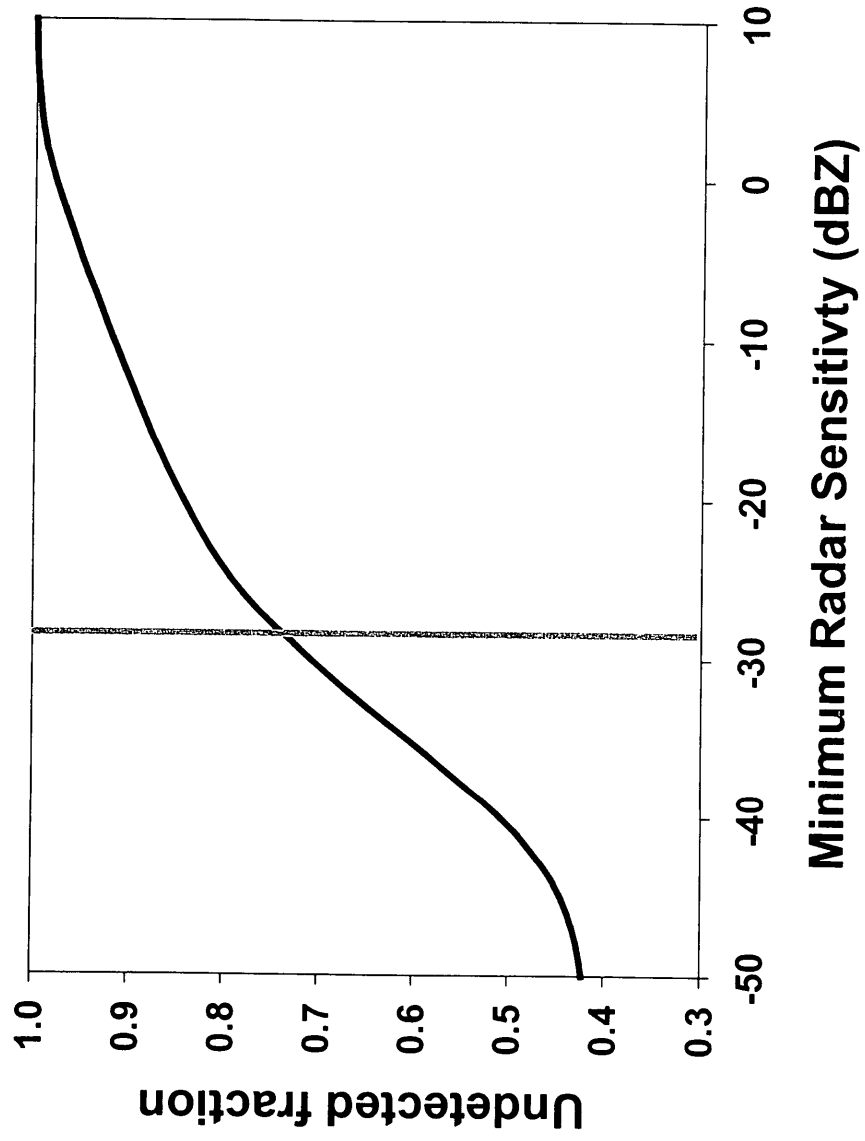


Fig. 9b

NAURU May - July 1999

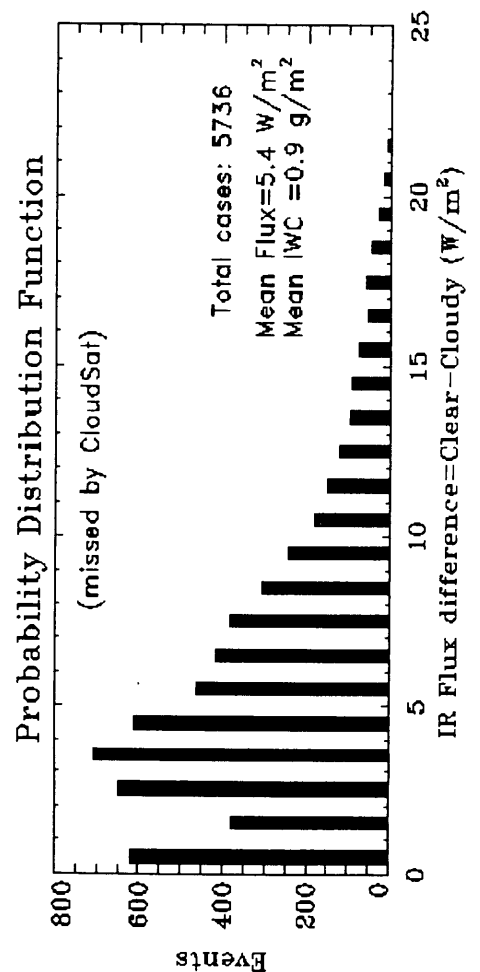
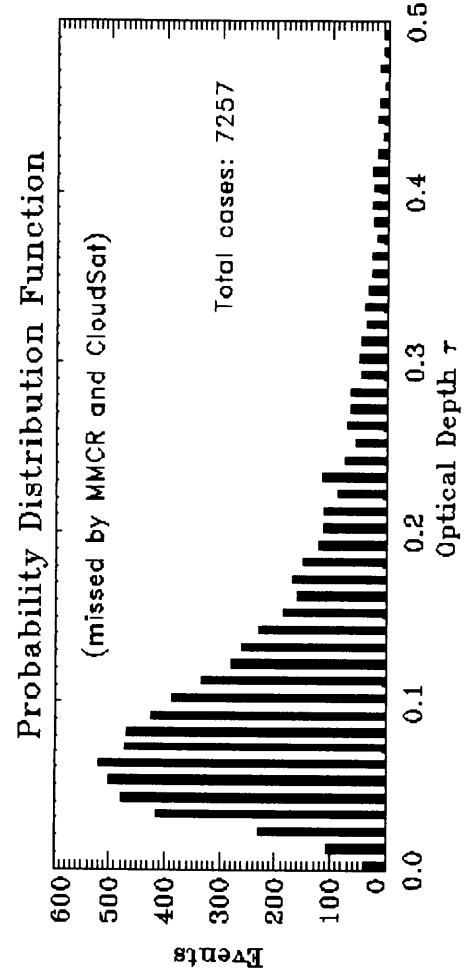
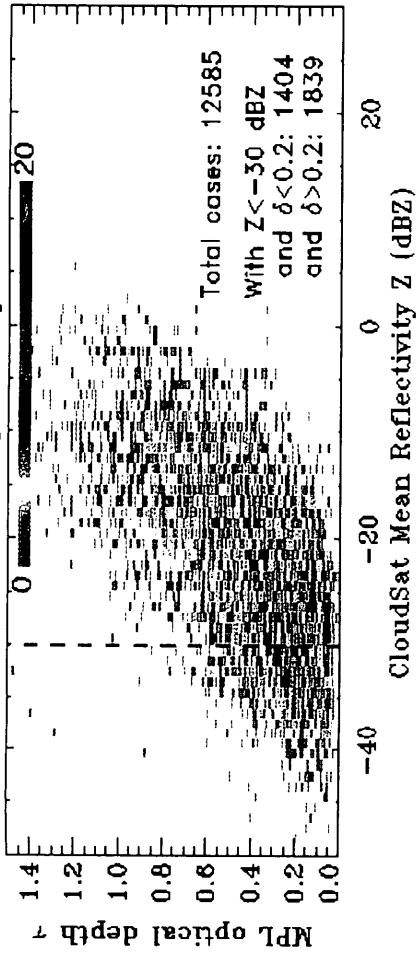


Fig 10

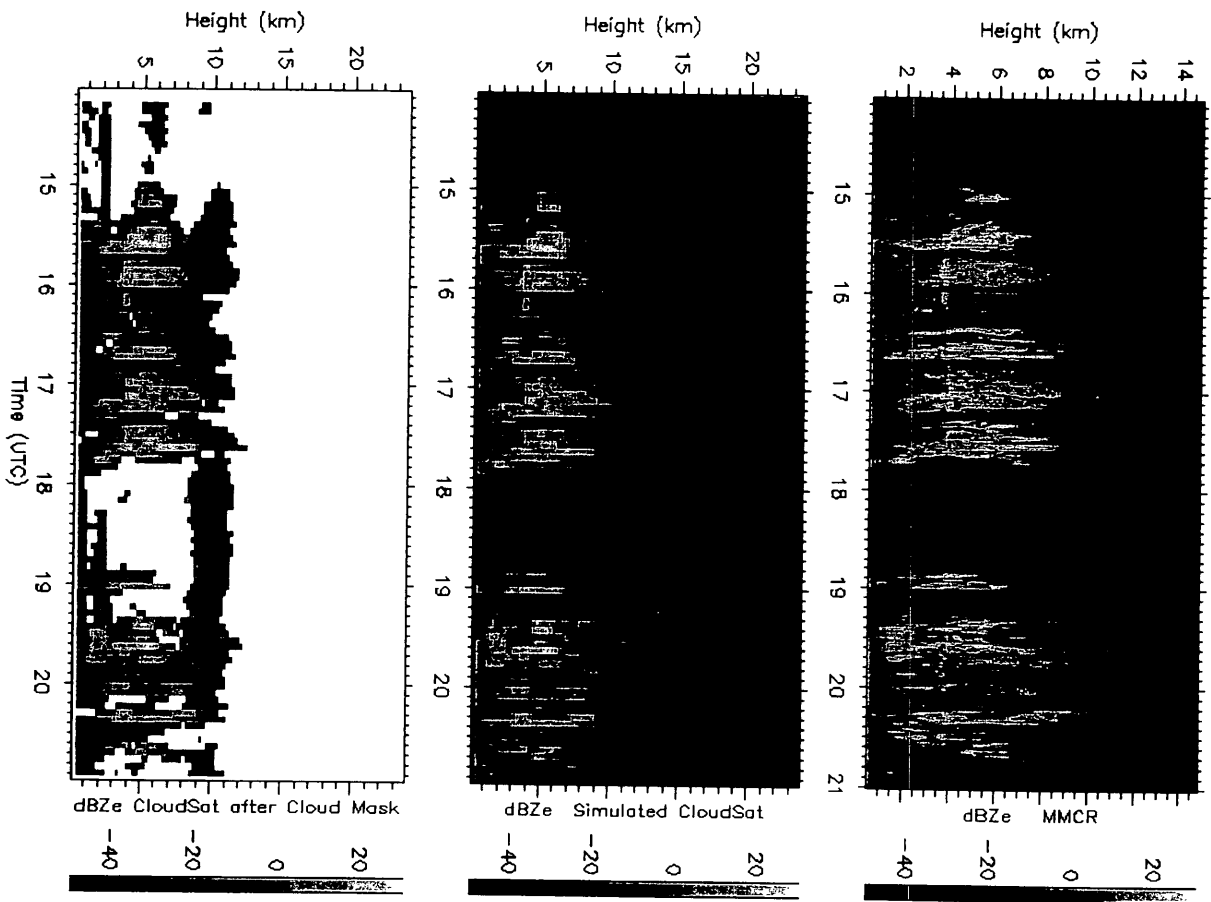


Fig. 11

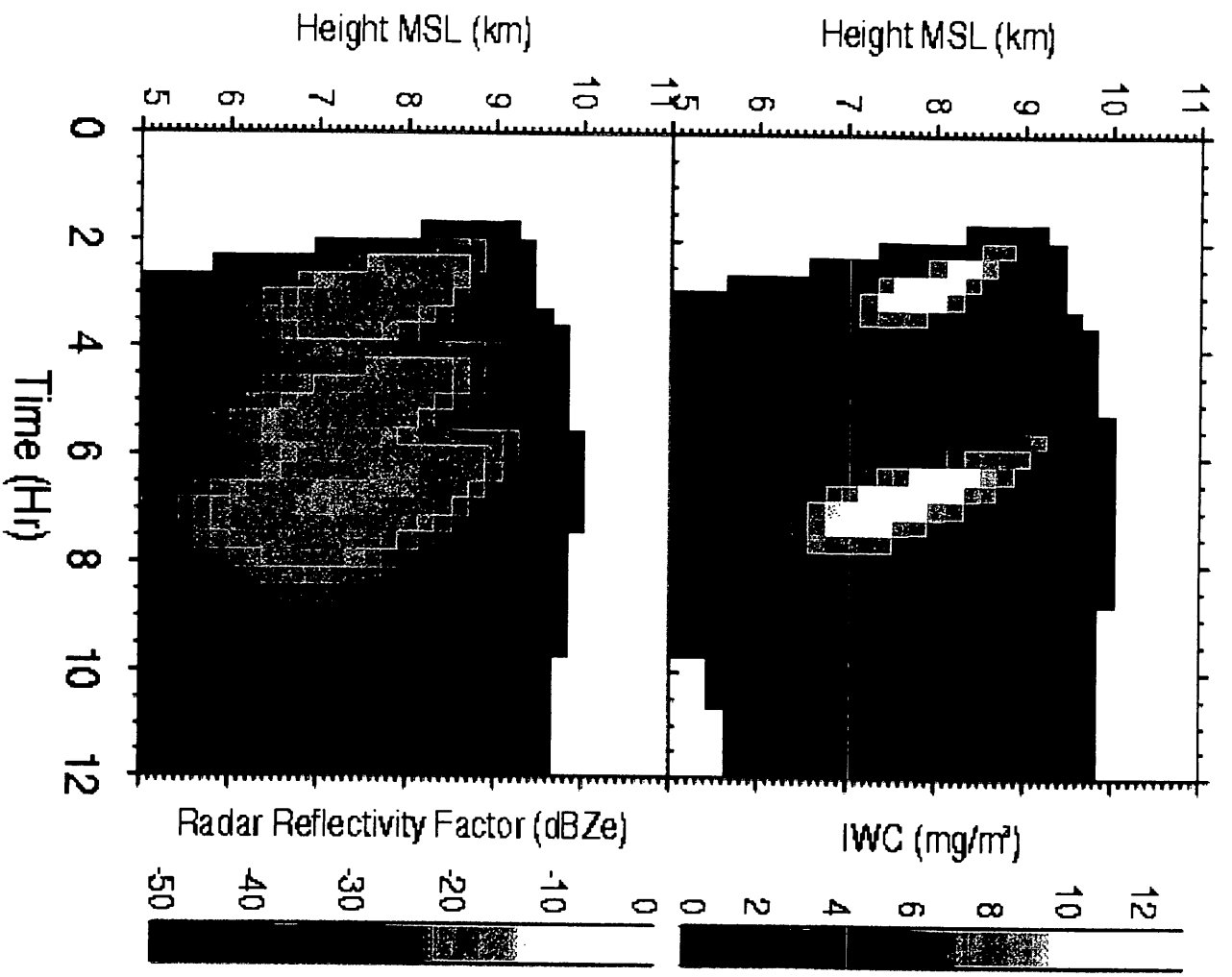


Fig. 12a

Ice Water Path g.m⁻²

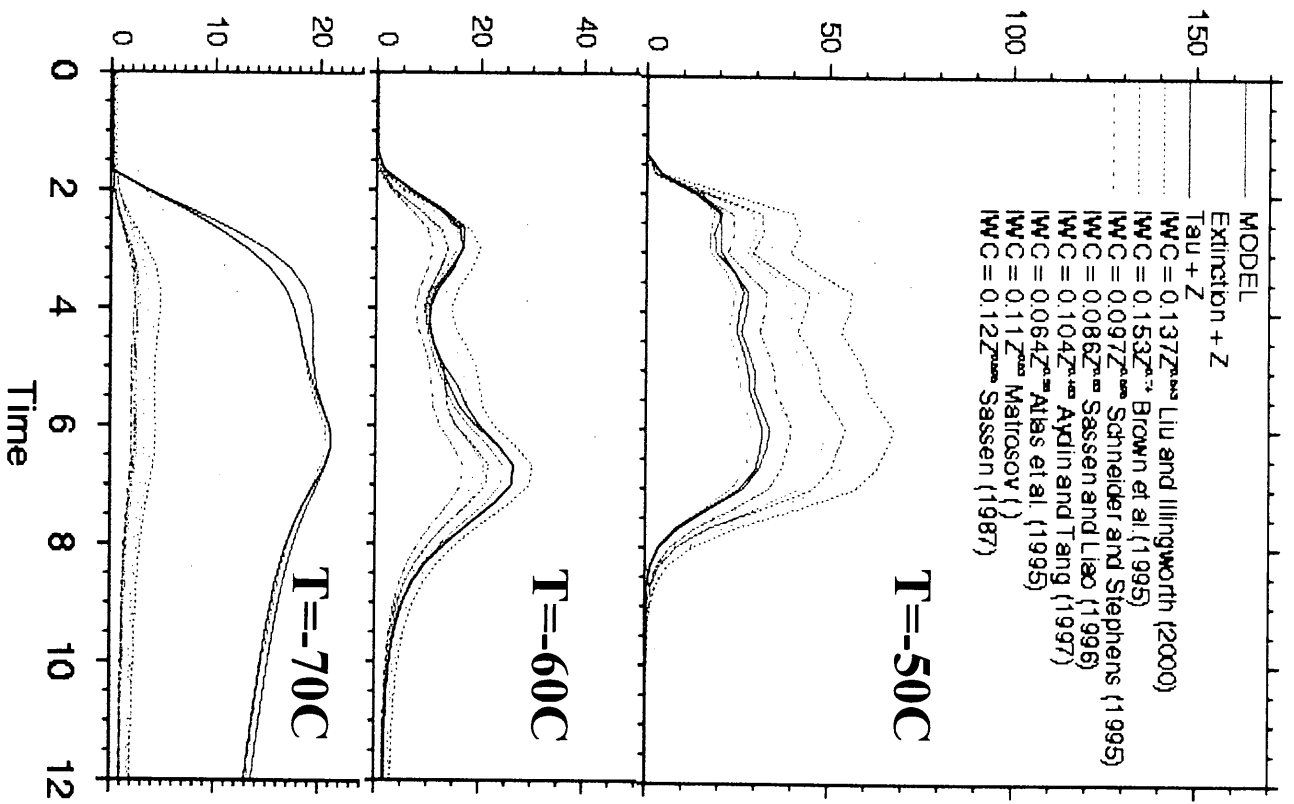


Fig. 12b